No. 2124

TECHNICAL REPORT

ELECTRICAL PROPERTIES OF RADIO FREQUENCY GLOW DISCHARGES IN AIR AT ATMOSPHERIC PRESSURE

by

H. A. Schwab
Weapons Development and Evaluation Laboratory

U. S. NAVAL WEAPONS LABORATORY
DAHLGREN, VIRGINIA

64

U. S. Naval Weapons Laboratory
Dahlgren, Virginia

NWL REPORT NO. 2124

ELECTRICAL PROPERTIES OF RADIO FREQUENCY GLOW DISCHARGES IN AIR AT ATMOSPHERIC PRESSURE

by

H. A. Schwab

November 1967

ABSTRACT

Gas discharges maintained by radio frequency power were examined in the frequency range 1-25 Mc/s. The discharges were maintained in air at atmospheric pressure between water cooled metal electrodes. The discharges were made symmetric by using two electrodes alike in shape and material.

Important discharge quantities such as the voltage necessary to maintain the discharge, current density, and dissipated power were measured. The minimum instantaneous value of voltage necessary to maintain a discharge was found to be 270 volts. The current density is largely independent of current and has a value of 30 amps/cm^2 (determined by using the peak discharge current). A minimum power of 4 watts is necessary to maintain a discharge.

The influence of current amplitude, frequency, electrode distance, and other parameters on discharge voltage and current density was examined. Both voltage and current density were found to be essentially independent of frequency in the frequency range considered.

Furthermore it was found that a number of properties of the type of discharge described in this report are analogous to the corresponding properties of dc glow discharges.

FOREWORD

The work described in this report was conducted under the Foundational Research Program of the Naval Weapons Laboratory. The report presents part of the results of an investigation of radio frequency gas discharges. Such discharges play a role in the problem area of "Hazards of Electromagnetic Radiation to Ordnance" (HERO). They occur when weapons are handled or loaded in high level rf fields, for example in the vicinity of a radiating antenna. By their capability to rectify or convert frequencies they add specific aspects to the general HERO problem.

This report was reviewed by the following personnel of the Weapons Development and Evaluation Laboratory:

L. J. Lysher, Head, Advanced Projects Group, Electromagnetic Hazards Division

J. N. Payne, Head, Electromagnetic Hazards Division

R. R. Potter, Assistant Director, Weapons Development and Evaluation Laboratory

D. W. Stoner, Director, Weapons Development and Evaluation Laboratory

APPROVED FOR RELEASE:

/s/ BERNARD SMITH
Technical Director

TABLE OF CONTENTS

LIST OF FIGURES

LIST OF FIGURES (continued)

LIST OF SYMBOLS

A	area
A_r	cross section of rod electrode
C	capacity
C_p	capacity in parallel to discharge gap
d	electrode distance
d_o	= 0.025 mm, unit of electrode distance settings
f	frequency
f_c	cut off frequency
f_m	= 25 Mc/s, maximum discharge frequency used
i	instantaneous value of current
I	amplitude of current
J	current density
l	length
λ	heat conductivity
P	power
Q	heat energy
R	resistance
R_s	current limiting resistance in series with discharge
t	time
T	temperature
ΔT	temperature difference between two points of an electrode
v	instantaneous value of voltage
V	amplitude of voltage
V_i	voltage necessary for ignition in each halfcycle
V_m	discharge voltage

LIST OF SYMBOLS (continued)

V_{pp}	voltage, peak to peak
Z_g	generator impedance
ω	angular frequency

I. INTRODUCTION

When weapons are handled or loaded in a radio frequency field, some of the power present in the field can be coupled into an electroexplosive device (EED) firing circuit and accidentally fire the EED. It has been reported previously that the voltage induced into the firing circuit can reach values high enough to maintain gas discharges (reference (1)). During the connection of a weapon umbilical cable, for example, a gas discharge may develop between two connector pins. It has also been shown that these rf gas discharges are capable of introducing rectification and frequency conversion. This capability constitutes a serious HERO (Hazards of Electromagnetic Radiation to Ordnance) hazard, since it renders the concept of EED protection by low pass filters ineffective. This Foundational Research Project was initiated with the aim of gaining some insight into the processes involved in these rf discharges.

The hypothesis followed in this investigation is that rectification is caused by changes in the discharge between glow discharge and arc mechanisms in alternate halfcycles. Such changes would introduce gross asymmetry between halfwaves of different polarity and would explain an efficient rectification. There is evidence that this mechanism of rectification does occur. It is this aspect which made it desirable to examine both glow type and arc type rf gas discharges separately to a certain extent. This report presents the results of an investigation of the glow type discharges. We will call these discharges "rf glow discharges", to indicate that important parameters of this type of rf discharge are closely related to those of glow discharges maintained with dc energy. However, we do not want to imply a complete equality of mechanisms in every detail. It is believed that the data presented in this report will justify to a certain extent the choice of the term "rf glow discharge". In addition some preliminary calculations of the ion and electron movements in dc and rf glow discharges indicate that the basic mechanisms are the same for both. Because of their preliminary nature, these calculations will not be discussed here.

It should be understood that this is not an investigation of rf glow discharges as such. The scope of the investigation is limited by its relation to the HERO rf discharge problem. For example, although it would be interesting to look into the influence of pressure variations upon discharge behavior, the HERO discharge problem is one of discharges in air at atmospheric pressure only. Therefore only discharges in air at atmospheric pressure were investigated. Some limitations on the range of other parameters (frequency range 1-30 Mc/s, power up to 400 watts, and standard connector materials) have already been pointed out in reference (2). Within these limitations this report presents a quantitative discussion of some of the characteristic electrical properties of rf glow discharges

II. DEFINITIONS AND PARAMETERS

Before entering the quantitative discussions, a qualitative description of the approach will be given.

The circuit used in the experiments is shown in Figure 1. A power source P (sinusoidal voltage waveform) delivers power to a series circuit consisting of a current limiting resistor R_s and the discharge gap. The discharge is ignited by touching the electrodes and then pulling them apart to a certain distance. With the discharge being maintained, instantaneous values of the voltage across the discharge gap and the current through the discharge are measured. (Photographs of waveforms obtained by this measurement will be discussed in Section IV.b and are shown for example in Figures 8 and 9, where the x-axis is time and y-axis is the instantaneous values of voltage in the upper waveform and the instantaneous value of current in the lower waveform.)

A typical waveform combination for one halfcycle is sketched in Figure 2. From such waveforms we can see the following:

a. Between t_1 and t_2 the voltage across the discharge gap is rising almost linearly with time. A constant but small current I_c is flowing during this period.

b. At time t_2 the voltage reaches the ignition point V_i and a large increase of discharge current occurs.

c. Between t_2 and t_3 the discharge carries a large current, which is determined by R_s and the voltage drop across R_s, which is of course the difference between the input voltage and the voltage across the discharge.

d. At t_3 the voltage falls below the minimum voltage necessary to maintain the discharge and the current decreases quickly.

e. Between t_3 and t_4 the current approaches zero and sometimes even assumes negative values. Since the discharge is symmetrical, the same sequence of events will take place in the negative halfcycle, with the polarity reversed.

In this report we will mainly be concerned with that part of the discharge which takes place between t_2 and t_3. As was indicated before we consider this part, which follows ignition at t_2 as a "dc glow discharge of short duration". We define the following quantities:

I_m = maximum value of current in interval $t_2 - t_3$

$$I_{av} = \frac{1}{t_4 - t_1} \int_{t_1}^{t_4} i\,dt$$ = average current in interval $t_1 - t_4$

V_m = the instantaneous value of the voltage at the time of occurrence of I_m

Under certain conditions the voltage will be constant in the interval t_2-t_3, but in general it is not.

For a definition of current density we must examine the appearance of the discharge. Take, for example, an rf discharge maintained between two plane parallel copper electrodes with a distance of 0 25 mm. Looking at this discharge through a microscope a distribution of light intensities as indicated in Figure 3a would be observed. This distribution is symmetrical with respect to the center plane Immediately at the surface of the electrodes we find a very thin layer of high light intensity and blue color. The edge of the area covered by this blue glow is very sharp and well defined. The size of the area grows with the discharge current, its shape being often but not always circular. The thickness of this blue glow in an axial direction is too small to be measured, however it is smaller than 0.025 mm Between these two blue layers on the electrode surfaces extends a space of faint pink glow The edge of this pink glow in a radial direction is not well defined, its intensity decreasing with distance from the discharge axis and gradually tending to zero. For a definition of current density we must define a discharge cross section. The blue glow naturally lends itself because of its well defined area. We therefore define the current density as the quotient $J = I/A$ where I = discharge current and A = area of electrode surface covered by the blue glow. Depending on which current we refer to we correspondingly define:

maximum current density $J_m = I_m/A$

average current density $J_{av} = I_{av}/A$

This is the discharge current density at the electrodes and is the only current density considered in this report. We further define "discharge frequency" as the frequency of the generator which produces the rf power maintaining the discharge. The frequency range investigated here is 1-25 Mc/s.

"Electrode distance", d, is the distance between the two closest points of a pair of electrodes, between which a discharge is maintained. When plane parallel electrodes are used this is equivalent to the discharge length.

III. EQUIPMENT

The quantities we want to measure are defined as points on the voltage and current waveforms (I_m, V_m). To measure these quantities we must display the waveforms, which have a high harmonic content. From a Fourier analysis of some of the waveforms it can be derived that a relation

$$f_c \geq 10\ f_m$$

is desirable (reference (2)), where f_c = cutoff frequency of the measuring system and f_m = highest discharge frequency. Thus for a maximum discharge frequency of 25 Mc/s, the cutoff frequency of the system should be 250 Mc/s. Thus the required properties of the measurement system can be deduced.

This bandwidth can only be handled by a sampling oscilloscope. A Tektronix Type 564 was used to display the voltage and current waveforms. The voltage across the discharge gap is in the order of 600 to 1000 volts peak-to-peak, which is above the range of this oscilloscope. A coaxial capacitive voltage divider was designed, capable of handling a frequency band from less than 1 Mc/s up to 250 Mc/s.

Coaxial techniques must be applied for these measurements because of shielding requirements. The discharge is maintained by approximately 800 V_{pp} and the oscilloscope input through the divider is 800mV_{pp}. Any spurious voltage coupled into the oscilloscope which does not pass through the signal voltage divider must be at least 30 db below the signal level. Since the signal itself is 60 db below the discharge voltage, the spurious signals should be kept 90 - 100 db below the discharge voltage. This of course requires careful shielding.

The construction of the electrode assembly is shown in Figure 4. Referring to this figure, parts (1) and (2) are electrode holders which hold the electrodes (3) and (4). These electrodes are changeable so that different electrode materials and shapes can be used. Holder (1) is fixed while holder (2) can be moved by turning the screw (5). This screw has a micrometer thread by which it is possible to set the elctrode distance with an accuracy of 0.025 mm. The capacitive divider is shown as part (6) of Figure 4. An essential feature of this divider is that the capacitive probe is embedded in solid teflon insulation. If the capacitive probe were to couple over an unprotected air gap, ions from the discharge region could drift over and cause a breakdown of this gap resulting in a discharge between electrode holder and capacitive probe.

The conversion of the discharge current into a proportional voltage which can be fed into the oscilloscope was achieved by a wideband current probe. This current probe has a transfer impedance of 1 ohm (1 volt output voltage into 50 ohm with 1 amp flowing through the probe). It is slipped over a wire connecting the electrode holder (2) to ground, as indicated in Figure 5 (System block diagram).

The energy dissipated in the discharge is in the order of 100 watts. This energy would quickly raise the electrodes and electrode holders to very high temperatures unless cooling were provided. A high temperature of these components is undesirable for several reasons. First, it would cause thermal expansion which would make a defined setting of small electrode distances impossible. Secondly, we want to avoid excessive oxidation of the electrode surfaces because this would change the discharge mechanisms. (Some oxidation cannot be avoided because of the presence of oxygen and the hot and chemically active discharge gas. However it can be held to a minimum by keeping the electrode surfaces at a constant low temperature). Finally, with special electrode forms such as rod shaped electrodes, which develop high temperature gradients, excessive heat would result in melting and deformation of the electrode shape. A water cooling system was therefore provided for effective cooling as shown in Figure 5. Plastic pipes and distilled water were used to prevent a current flow through the water due to the potential difference between the two electrodes. The dc resistance of the water between the two electrodes was measured to be >20MΩ.

The resistors used for limiting the discharge current were high frequency resistors with a 50 watt power rating. Shielding was provided by enclosing them in an aluminum box. Since they were used for dissipating more than 50 watts in this case, they were cooled by forced air.

The power necessary to maintain the discharge is generated by a Navy URT-3 transmitter, capable of producing 500 watts in the frequency range 2 to 25 Mc/s, and a power amplifier, capable of producing 400 watts in the frequency range 1 to 10 Mc/s. The URT-3 must be terminated with a 50 ohm load; therefore, a matching network was inserted between it and the current limiting resistance.

The frequency behavior of this measuring system will now be considered. The frequency response of the voltage channel was measured by applying a constant sinusoidal voltage at point A in Figure 5 and monitoring the oscilloscope response. The result of this measurement is shown in Figure 6. From 10 Kc/s to 125 Mc/s the response is constant. Between 125 and 250 Mc/s it increases by less than 1 db. The voltage waveform displayed at the oscilloscope screen can therefore be considered identical to the waveform actually present between the electrodes.

The frequency response of the current channel was not as good as the response of the voltage channel, although the current probe

by itself has an upper frequency limit (3 db) of 260 Mc/s. The difficulty is that the current flowing through the probe is not identical to the discharge current. This can be seen from Figure 7, in which point A corresponds to the electrode. The electrode holder has a stray capacity C to ground which is in parallel with the inductance L of the wire through the current probe. With I_d= discharge current, I_c = current through the stray capacity and I_p = current through the probe we have:

$$I_c \cdot \frac{1}{j\omega C} = j\omega L\, I_p$$

and

$$I_d = I_c + I_p$$

This results in

$$I_p = I_d \cdot \frac{1}{1-\omega^2 LC} = I_d \cdot \frac{1}{1-\left(\frac{\omega}{\omega_R}\right)^2}$$

where

$$\omega_R = \frac{1}{\sqrt{LC}} \quad ;$$

This means that the response of the current channel will rise with frequency. The measured response is shown in Figure 6. Its rise is a combined effect of current probe frequency response and the resonance effect. This frequency response will raise the amplitudes of the harmonics of 25 Mc/s by the following factors:

FREQUENCY	FACTOR
f_1 = 25 Mc/s	1.0
f_3 = 75 Mc/s	1.0
f_5 = 125 Mc/s	1.1
f_7 = 175 Mc/s	1.25
f_9 = 225 Mc/s	1.45

Only the highest order harmonics are significantly affected. Fortunately, they are small in amplitude and a small error does not affect the results appreciably. Also, this influence is noticeable only at the highest discharge frequencies.

The linearity of the current probe was checked to make sure that the ferrite it contains did not introduce distortions of the transformed current waveform. Up to 2 amps peak current, no deviation from linearity could be found.

Both waveforms, voltage and current, are conducted via coaxial cables from the discharge to the oscilloscope. It is necessary to keep the difference between the time delays introduced by these cables to a minimum, to ensure that the two waveforms displayed at the oscilloscope are properly time related. By adjusting the cable lengths to proper values the time difference between the two displayed waveforms was kept below $5 \cdot 10^{-10}$ seconds.

IV. MEASUREMENTS AND RESULTS

a. General

The discharges were ignited by touching the electrodes together and then pulling them apart. Only at very small electrode distances is the available voltage high enough to cause ignition by breakdown. (Approximately 400 V_{rms} are necessary to cause the breakdown of a 0.025mm gap).

The appearance of a discharge under the microscope was described in Section II. It should be noted here that it looks almost exactly like a dc glow discharge with the exception that the rf discharge is symmetrical. The symmetry is caused by the continuous change of the electrode function from cathode to anode and back. A sketch of how an rf discharge looks is given in Figure 3. Photographs of dc glow discharges at atmospheric pressure in air can be found in references (3) and (4).

Usually, the position of the discharge on the electrodes is fixed and is between the parallel front areas of the electrodes as indicated in Figure 3a. In some cases, however, it is unstable. The discharge may move very quickly from one position to another, with such a high speed that the eye cannot follow it. The positions which the discharge assumes under these conditions are not restricted to the face area of the electrodes. The periphery may also be included such that the blue glow is in part on the face area and in part reaches around to the cylindrical part of the electrode surface.

This instability of position usually is accompanied by two other phenomena: a loud hissing noise and an instability in voltage. For example, at 1 Mc/s and d = 0.5 mm, V_m continuously changes between 380 and 410 volts. At times the discharge maintains the periphery position as a fixed position (Figure 3b). V_m is then usually higher than for a center position (at the same electrode distance), the difference being in the order of 10%.

Such conditions typically exist at 1 Mc/s and $d \geq 0.25$ mm and sometimes occur at 2 Mc/s but not at higher frequencies. At 1 Mc/s for d = 0.25 mm and greater, the noise produced by the discharge increases with electrode distance until suddenly the discharge stops altogether. Using plane parallel copper electrodes and the available power it was not possible to maintain a discharge at 1 Mc/s and $d > 0.6$ mm.

Neither the noise nor the tendency of the discharge to change position was found with discharges operated at frequencies of 5 Mc/s or above. Also, the discharge could be maintained at electrode distances up to 2.5 mm with no difficulty. (The electrode distance could not be increased beyond 2.5 mm because of mechanical reasons).

The values of V_m given in this chapter for 1 and 2 Mc/s are the minimum values obtained whenever an instability of position and voltage occurred. The value of V_m may be higher than the minimum value by up to 10% under certain discharge conditions.

Prior to each measurement the electrode surface was cleaned by filing. After the discharge had been maintained between two freshly cleaned electrodes for some time a deposit formed on them. For copper electrodes this deposit had the appearance of a black paste. The amount of deposit depended on how long the discharge was maintained, but it could be seen in a matter of seconds. After approximately one minute a saturation was reached and the amount of deposit did not essentially increase even when the discharge was maintained for an hour.

The following discussions in this section apply to plane parallel copper electrodes, unless otherwise stated.

b. Typical Waveforms

In this section typical waveforms and their dependence on several parameters will be shown in photographs of waveform oscillograms. The oscillograms are grouped by frequencies. Each of them, Figures 8 to 11, shows one frequency. In each photograph the upper waveform represents voltage on a scale of 200 volts per major division (1 cm at the oscilloscope screen). The lower waveform represents current on a scale given for each photograph. With the exception of Figure 8e a peak current of 0.3 amps is shown in the left column of photographs and a peak current of 0.8 amps in the right column. The electrode distance d is given for each photograph in units of $d_o = 0.025$ mm, i.e., $d = 2d_o$ represents an electrode distance of 0.05 mm.

The photographs show the influence of several discharge parameters upon the discharge waveform. Some of these influences will be discussed in detail in the following sections. However, let us first discuss two phenomena which are obvious from the photographs but are not mentioned elsewhere in this report. One is the interval of nearly constant current preceding the rise of the discharge current to its

peak value in every halfcycle. This is the interval marked t_1-t_2 in Figure 2. It is clear from Figures 6 - 11 that the amplitude of this current I_c relative to the peak current I_m increases with frequency. It is almost 50% of maximum current at 25 Mc/s whereas it is hardly detectable at 1 Mc/s. Since this current is constant during a period of approximately linear increase in voltage we can conclude that it is probably a current charging a capacity. It cannot, however, be explained as being the current charging the capacity present between the two metal electrodes in the absense of a discharge. This electrode capacity would result in a considerably lower charging current. The major portion of this current results from building up the space charges in front of the cathode in each halfcycle. These space charges are necessary for the formation of the cathode fall region. The cathode fall region must be built up in every halfcycle and this results in a considerable transportation of charges. Conclusions can be drawn from the size of this charging current about some properties of the cathode fall region, but this will not be discussed in this report.

A small variation of very high frequency is superimposed on the current I_c in Figure 11. This is not a discharge property. The frequency is approximately 400 Mc/s and was introduced by the resonance in the current channel discussed in section III.

The second phenomenon to be mentioned here is the ignition voltage V_i which is necessary to start the discharge current in each halfcycle. This voltage is small for small d, rises to a maximum for medium d and then decreases for large d. For example, it can be seen from Figure 8 that V_i = 360 V for d = $2d_o$, V_i = 400 volts for d = $2.5d_o$, and V_i = 340 volts for d = $8d_o$. For large d, V_i usually is not the maximum voltage value in one halfcycle but v rises after ignition, thus $V_m > V_i$.

There are some changes in the discharge waveforms with frequency. For example, the voltage waveform seems to gradually approach a sinewave at the high frequencies. While this is obvious from the photographs one cannot conclude that it is a discharge property. The electric circuit associated with the discharge also has an influence on the waveforms and some of the changes in waveform with frequency can be attributed to this circuit influence. This will be discussed in the following section.

For taking the photographs the calibration of the oscilloscope was adjusted to correct the parallax error. So the faint grid pattern produced by reflection from the oscilloscope screen which might be seen on some of the photographs has to be disregarded.

c. Influence of Circuit Upon Waveforms

For a discussion of the term "circuit" we refer to Figure 12. There the minimum number of circuit elements involved in producing and maintaining an rf discharge is shown. We must have a generator with internal impedance Z_g, a current limiting resistor R_s in series with

the discharge, the discharge gap G and undesired stray capacity C_p in parallel with the discharge. We will always choose R_s such that the condition $R_s >> Z_g$ is fulfilled, so that we impress a sinusodial voltage on the terminals a-a'. In this case Z_g will have no influence on the discharge waveforms and we can assume $Z_g = 0$ for the following discussion. The "circuit associated with the discharge" then consists of the resistor R_s and the capacitor C_p.

R_s is obviously a necessary circuit element. As can be seen from the waveforms discussed in the preceding section, the discharge voltage does not change very much with current, at least for small d and low frequencies. This means that the discharge, once it is ignited, has a very low impedance. Therefore the resistance R_s is necessary to allow a defined adjustment of discharge current. Only real resistances R_s are considered in this report.

The influence of R_s on the discharge waveform will become immediately clear when considering the two extreme cases, $R_s \to 0$ and $R_s \to \infty$. If R_s were zero this would be equivalent to impressing the generator voltage waveform, a sinusoid by definition, upon the discharge gap. We must limit the peak voltage to a value only slightly above the required minimum (V_{min}). Then the current can only flow during a very short period, as long as $V \geq V_{min}$. Since the voltage waveform is sinusoidal, the voltage will drop below that minimum soon after reaching its peak value and the current will stop. The resulting approximate current waveform is shown in Figure 13a. In the other case, $R_s \to \infty$, we force a sinusoidal current through the discharge. The voltage then will approximately assume a shape as shown in Figure 13b, reaching the ignition voltage as soon as the current flow begins and, at least for small d, approximately holding the value V_m for the period of sustained current flow which is the full halfcycle in this case. We will now estimate what $R_s = 0$ and $R_s = \infty$ mean in practical terms. Figure 14 shows that the sinusoidal voltage maintained at the terminals a-a' (Figure 12) always is a sum of the voltage over the discharge gap plus the voltage drop over R_s caused by the discharge current: $V_i = V_d + V_R$. If $V_R << V_d$ we have essentially the sinusoidal input voltage on the discharge gap. If $V_R >> V_d$, the major portion of the input voltage is applied across R_s, resulting in an almost sinusoidal current, since an almost sinusoidal voltage is applied across the linear elements R_s. If we define a "discharge impedance" by $R_d = V_m/I_m$, with $I_m = 0.5$amp and $V_m = 300$V we get an $R_d = 600\Omega$. $R_s >> 600\Omega$ will then approach $R_s = \infty$ and $R_s << 600\Omega$ will approach $R_s = 0$.

Figures 15 a, b, and c show the waveforms obtained for $I_m = 0.5$ amp and $R_s = 100\Omega$, 500Ω and 2000Ω respectively, using plane parallel electrodes, d = 0.125mm, at 1 Mc/s. From these photographs it can be seen that $R_s = 100\Omega$ approximates $R_s = 0$ and $R_s = 2000\Omega$ approximates $R_s = \infty$ as expected from the preceding discussion.

For the purpose of discharge measurements R_s should not be too small, because a small R_s results in a discharge which is not very stable. Nor should R_s be too large, because then most of the available power will be consumed in R_s and high discharge currents cannot be obtained. For most of the measurements R_s = 500Ω was chosen for these reasons.

The second element in the discharge circuit is the stray capacity parallel to the discharge. Ideally, this capacity should be zero; in the equipment used for the measurements it is C_p = 25pF. The effect of C_p on the discharge is that it provides a reservoir of charges in parallel to the discharge. With i_d the current through discharge, i_R the current through R_s and i_c the current into the capacitor we have

$$i_R = i_d + i_c ;$$

i_c may be positive or negative, depending on the direction of change of voltage across the capacitor. At least with small electrode distances the voltage usually drops slightly after ignition. In these cases the effect of the capacitor is to momentarily increase the discharge current. To analyze exactly what is going on in the discharge as a consequence of the presence of C_p is a very complicated problem. The details of these processes, however, are not of interest here. We are interested in determining the amount of distortion introduced by a certain C_p and the limitations of the measurements caused by this interference. Figure 16 shows waveforms at 1 Mc/s for various values of C_p. The value of C_p given is the total capacity, the sum of the actual stray capacity (25 pF , which cannot be removed) and an additional capacitor placed in the circuit. Up to 125 pF the distortions are tolerable and the value indicated for V_m is the same on all three photographs. The waveforms obtained for C_p = 225 pF and C_p = 425 pF show a much higher degree of distortion and yield a V_m reading which is approximately 10% too high. So 125 pF seems to be the limit of C_p tolerable at a frequency of 1 Mc/s.

It is natural to expect that a lower value of C_p would be sufficient to cause the same effects at higher frequencies. This is shown in Figure 15 (d-f) for 5 Mc/s. By comparing Figure 15d with Figure 16c one can see that 125 pF has the same effect upon the waveform at 1 Mc/s as does 25 pF at 5 Mc/s. Since the stray capacity is fixed at 25 pF , the distortion introduced by it will increase with frequency and at 10 Mc/s will be the same as found for 250 pF at 1 Mc/s. This means that with the presently available system no undistorted waveforms can be recorded at frequencies greater than 5 Mc/s. We find however, that the waveforms obtained at higher frequencies with C_p = 25 pF are very similar to those found at lower frequencies for proportionately bigger C_p. From this we conclude that the different waveforms we get at the higher frequencies very likely are not due to different discharge behavior at these frequencies but rather caused by the influence of the stray

capacity C_p. If equipment with sufficiently small C_p ($\leq$ 5 pF) were available, we would probably obtain essentially the same waveforms at all frequencies between 1-25 Mc/s.

This statement does not apply to the capacitive current I_c which flows before ignition. This part of the current waveform increases in amplitude with frequency. (The amplitude of I_c provides a method of identifying the frequency at which a certain current waveform was obtained. Figure 15d and Figure 16c, for example, show almost the same current waveform for 1 and 5 Mc/s, with the exception of the amplitude of I_c.)

The presence of C_p has another consequence too. At 25 Mc/s the reactance of the 25 pF is 250Ω. R_s and C_p form a voltage divider which allows only a fraction of the input voltage to build up over the discharge gap. With R_s = 500Ω at the available power level the voltage was not large enough to maintain a discharge. Therefore R_s = 300Ω was used for the measurements at 25 Mc/s.

d. Discharge Voltage (V_m)

V_m was defined as the instantaneous value of the voltage at the time of occurrence of I_m (section II). In this section the measurement technique and the influence of several parameters on V_m will be described.

1. Measurement Method and Accuracy

The voltage waveform was displayed on the screen of the sampling oscilloscope. V_m was read directly from the screen. The reading accuracy was ±5 volts. (corresponding to approximately ±2%).

The absolute calibration of the voltage channel was performed by applying an rf voltage of known amplitude to the electrode holder (1) (Figure 4) and adjusting the oscilloscope gain. By this method the voltage channel is calibrated as a unit. The equipment used for setting the amplitude of the calibration voltage has an accuracy of ±3%. Combined with the reading error this results in a maximum deviation of the measured value from the true value of ± 5%. Calibration was regularly checked.

I_m was also read from the oscilloscope screen. The current amplitude is not as critical as the voltage amplitude; therefore the current channel was not calibrated as acturately. It is estimated that the deviation of the measured current from the true current was less than ±8%.

2. Influence of Various Parameters on V_m

(a) Time

The discharge voltage varies with time even when all other parameters are kept constant. The reason for this dependence on time is not clear. It is likely, however, that the oxide layer which develops on the electrode surface covered by the discharge is responsible for it. Typical measurements of V_m as a function of time with all other parameters being constant are shown in Figure 17. Time $t = 0$ represents the time of ignition of the discharge. The current was changed during the measurement between two levels, 0.4 and 0.8 amps. For this measurement the electrode surfaces were cleaned by filing, so that at $t = 0$ there was no oxide layer. This layer, however, develops quickly while the discharge is maintained. (Under the microscope it can be seen that the oxide layer is only a faint darkening after a discharge time of a few seconds, but it accumulates to a black layer of up to approximately 10^{-2} mm thickness after discharge times of a few minutes).

The measurements show that V_m varies roughly exponentially, and after a certain time approaches a stable value if the current is kept constant. A change in current will have two effects. First, there will be a change in voltage which takes place immediately; second, the voltage associated with the new current will again vary with time until it approaches a constant value. The time necessary to reach that stable value depends on both the current amplitude and the "history" of the electrode, i.e., how long the discharge was on before. It is of the order of several minutes. The total range of V_m associated with a particular current level depends on this level and is higher for low currents. The maximum variation observed was 10% at a current of 0.4 amps.

(b) I and R_s

It is obvious from the measurement shown in Figure 17 that V_m depends on the current amplitude I_m. It is also obvious that the change ΔV_m which is caused by a change ΔI_m depends on time. Long time influences were discussed in the previous paragraph (i.e., times in the order of 10 minutes). In this paragraph only such changes of V_m shall be discussed which follow the current immediately, "immediately" meaning times in the order of seconds. The determination of the amount of this effect of I_m on V_m has to be done very carefully, since it is in the same order of magnitude as several other effects. First there is the time influence on V_m which was discussed in the previous paragraph. To eliminate this as much as possible we make use of the result that V_m is most stable for high currents. So we maintain the discharge at a current level of 0.8 amps most of the time and only change to other levels (0.5 amps and 0.3 amps) for the time necessary to read V_m. After each reading we set I_m back to 0.8 amps. Secondly the change of V_m is in the order of the reading

error Therefore several readings were taken at one point (d = constant), the average value of which was taken as the result. The results obtained by this method are shown in Figures 18-20 as a function of electrode distance for three frequencies. An increase in current results in a decrease of voltage V_m, the magnitude at small d being approximately 3% of V_m for each step of current amplitude from 0.3 to 0.5 to 0.8 amps

The result in the previous paragraph describes the changes of V_m within seconds after a change in I_m but does not apply for V_m obtained after longer times or for very short times. Within any half cycle the instantaneous value of the voltage never decreases with rising current. Usually the voltage is highest when the current is at its peak, sometimes the voltage is constant through the period of current flow (Figure 8a), but it does not decrease with increasing current. Most likely the effect of I_m on V_m is due to temperature changes in the discharge plasma caused by changing current amplitudes Because of the heat capacity of the plasma, the current will be related to the average termperature during each one half cycle at the frequencies of interest here. After seconds however, the plasma temperature can adjust to a new current level and result in a different V_m.

Turning to the influence of R_s on V_m, we showed previously (Figure 15) that R_s has a strong influence on the current waveforms. For the same peak current I_m, therefore, different R_s will result in different average currents I_{av} and thus in different heating of the plasma From this we would expect large values of R_s to yield a lower value of V_m than small R_s. This is indeed the case as shown in Figure 19 a, b and c.

(c) Electrode Distance d

The influence of the electrode distance on V_m is shown in the graphs Figures 18-20. V_m always increases with increasing d. The rate of increase depends on d and is greatest for small d. Thus we read = 7000 V/cm at $d/d_0 = 2$ and = 1400 V/cm at $d/d_0 = 20$ from Figure 19. The most significant property of the V_m-d relation is that V_m does not tend to zero when d approaches zero. There is a minimum V_m even at very small d The smallest d which could be set for these measurements was approximately 0.02 mm At d smaller than that the discharge has a tendency to build up material on the electrode surfaces which forms a conductive bridge between the electrodes within seconds (reference 3). When this conductive bridge shorts the electrode gap the discharge stops of course. For this reason it is not possible to measure V_m at d less than 0.02 mm. The only possible measurement is to gradually decrease the electrode distance, taking the voltage reading just before shorting as the minimum V_m. By this method a minimum value of 270 V is found for V_m, for frequencies 1-5 Mc/s

(d) Electrode Material

It is well known that in a dc normal glow discharge the voltage necessary to maintain the discharge in general depends strongly on the cathode material. In references (5) and (6) the following normal cathode fall voltages for several materials in air are given as:

Au 285 V
Cu 370 V
Fe 269 V
Ni 226 V

From this we would expect that different electrode materials would yield different values of V_m in rf discharges when all other parameters are kept constant. Experiment shows, however, that different electrode materials yield V_m values much closer together than one would expect from the cathode fall values listed. To determine whether this effect is a particular property of rf discharges, measurements at dc were made with the same cathode materials. These measurements were made at d = 0.05 mm. The results, in volts, are in the following table:

	I = 0.1 amp	I = 0.2 amp
Au	312	313
Cu	285	287
Fe	285	295
Ni	300	285

This shows that the cathode fall voltages measured at low pressures do not apply for atmospheric pressure (similar results in reference (4)) and, second, that at atmospheric pressure the cathode fall voltages for different cathode materials vary much less than they do at lower pressures. It is not surprising then, that for rf discharges at atmospheric pressure the variation of V_m for different electrode materials is small also. The variation, however, is there and can be measured.

For demonstration of this effect, an rf discharge was maintained between two different electrodes, one of gold, the other one of copper . These two materials show a difference in voltage of ≈9% at dc. If there is a correspondence between the voltage measured across a dc discharge and the V_m of an rf discharge, then we should expect V_m to be higher in the half wave in which the gold electrode is the cathode. This indeed is found to be true and is shown in Figure 21. To take these photographs the film was exposed twice, first to record the waveform, second to establish an accurate zero voltage reference line. (a dc component had to be measured here and the capacitive divider system used for all symmetrical discharge measurements could not be used.) In Figure 21(a) the copper electrode is cathode for the negative half cycle, the gold electrode for the positive one. The upper half cycle yields a V_m which is 5% higher than the

one of the lower halfcycle. The difference of the two values for V_m is so small that it might have been due to the nonlinearity of the oscilloscope trace deflection. To exclude this possible error the positions of the two electrodes were exchanged and the result is shown in Figure 21(b). Here again V_m is higher for the half wave in which Au is the cathode, which is now displayed in the lower half of the screen. This time the difference was 10%; so we conclude that the real difference is the mean of the two measured values, being ≈ 7.5%.

For combinations Cu-Fe and Cu-Ni no difference in V_m for different polarity half waves could be measured.

(e) Frequency

In Figures 8-11 typical waveforms for the frequencies 1, 5, 10, and 25 Mc/s are shown. It is obvious from the voltage waveforms that the frequency has only a small effect on V_m if any at all.

Since we are looking for a small effect we will compare only the V_m values at 1, 2, and 5 Mc/s. At higher frequencies, the circuit introduces distortions into the waveforms as discussed in section IV, (c).

A statistically designed measurement series was made.* The following variables and levels were chosen:

two current levels: 0.5 and 0.8 amps
two distance levels: 0.125 and 0.375 mm
three frequencies: 1, 2, and 5 Mc/s
five time durations: 0, 1.5, 3, 4.5, and 6 minutes after ignition

Five replications were made.

The average values of V_m obtained for these measurements are as follows:

f →		1 Mc/s	2 Mc/s	5 Mc/s
d=0.125mm	0.5Amp	328.0	329.7	311.9
	0.8Amp	314.6	314.9	303.4
d=0.375mm	0.5Amp	382.5	365.0	343.7
	0.8Amp	348.6	348.4	330.0

* Mr. Roger W. Carson gave valuable assistance in the design and analysis of this measurement series, which is gratefully acknowledged.

The standard deviation in this measurement was found to be ±6.2 volts. The result shows that the V_m values obtained for 1 and 2 Mc/s are not significantly different, whereas the ones for 5 Mc/s are approximately 5% lower.

(f) Electrode Shape

The absolute values of V_m of two different electrode shapes cannot easily be compared because of the difficulty of defining the discharge length. For plane parallel electrodes it is well defined and constant for all parts of the current. For cone shaped electrodes, however, we have different "lengths" of the discharge, depending on which part of the current is under consideration. The small portion of the total discharge current which flows from point to point of the electrodes finds a smaller length than other parts flowing between areas further away from the point of the cone. So when changing the electrode shapes we will in general change the discharge length also and it is difficult to define an equivalent length for every electrode shape For this reason we will not compare absolute values of V_m for different electrode forms ,but rather compare the change of V_m with I_m.

For plane parallel electrodes it was found that an increase in I_m results in a decrease of V_m. This is not true for all electrode shapes. For the cone shaped electrode shown in Figure 22 (c) for example, V_m increases with I_m. This is easy to visualize, since each current fraction added to the already existing current must flow over a longer distance from one electrode to the other. So when increasing I_m, the average discharge length is simultaneously increased. (Since $\Delta V_m/\Delta I_m<0$ for plane parallel electrodes and $\Delta V_m/\Delta I_m>0$ for a cone shaped electrode with cone angle 40°, there should be a cone angle which yields $\Delta V_m/\Delta I_m = 0$).

Similar considerations are true for the shape shown in Figure 22 (b). The electrode is a cylinder of 1 mm diameter. In this case V_m also increases when I_m is increased beyond the value which just covers the circular area at the end of the rod. Some results of measurements on different electrode forms are plotted in Figure 23.

e. Current Density (J)

The definition of current density J_m as given in section II, is $J_m = I_m/A$. Here I_m is the maximum current in one half cycle and A the area of the electrode surface which is covered by the blue glow. In the following section the measurement method and the influence of several parameters on J will be discussed.

1. Measurement Method and Accuracy

Two quantities must be measured to determine J_m: the area A of the blue negative glow, and the peak current I_m.

The negative glow area A was measured under a microscope. For plane parallel electrodes the width of this glow in a direction perpendicular to the direction of current flow was measured. The area is assumed circular and the measured width to be the diameter. In general, however, the area covered by the negative glow is not round and this assumption leads to inaccurate results. The fact that the position of the discharge on the electrode surface varies is another source of error with plane parallel electrodes. Sometimes this variation is perodic between one place and another. The change of position may occur so quickly that the eye cannot distinguish between different positions and one gets the impression that the discharge covers both areas simultaneously. Thus the diameter of the discharge appears to be greater than it actually is. The movement of the discharge position depends on the electrode distance d. At some distances the discharge position is rather stable, at others it varies more. By varying d and measuring the minimum discharge diameter one can usually find the true discharge cross-section.

A better method, however, is to use a different electrode form. With plane parallel electrodes, the position of the discharge is rather arbitrary, as long as the discharge diameter is smaller than the diameter of the plane parallel electrode surface. The discharge has no preferred position on the electrode surface. By choosing a different electorde shape, however, we can stabilize the discharge position. With conical electrodes for example the discharge position will be in the vicinity of the cone points, because this position results in the shortest discharge length and smallest voltage. By knowing the geometry of the cone and measuring the length of the cone covered by the discharge under the microscope one can calculate the discharge area. Some uncertainty remains about the discharge area even here because the portion of the cone surface covered by the discharge is not exactly symmetrical about the axis. So the length of the discharge covered cone portion must be estimated. However, the discharge area can be determined within $\pm$ 10% for I_m greater than 0.5 amps. Also it is assumed that the observed area is the peak instantaneous area. In reality the observed area value may lie somewhere between the peak and average values.

The peak current was read from the oscilloscope. The accuracy of this reading was $\pm$ 8%, so the error in the final value of J_m may be as great as $\pm$ 18%.

2. Influence of Various Parameters on J

(a) Current

When measuring the area covered by the discharge as a function of peak current I_m we obtain results as shown in Figure 24. These results show an almost linear relationship between A and I_m. The slight deviation from linearity is well within the error limits as discussed before. So within the accuracy limits of this measurement we find that A is directly proportional to I_m and that J_m is a constant with respect to I_m. From the graphs (Figure 24) we determine a mean value of 30 amp/cm^2 for J_m.

(b) Waveform

We had chosen the peak value of the current waveform to define current density. This choice was made for convenience of measurement. We will now consider the question of whether A depends on the waveform when I_m is kept constant. The most convenient way to influence the waveform is to change R_s.

Measurements were made with R_s = 100 ohms and R_s = 1 kΩ at both 1 and 5 Mc/s. The results are shown in the following table.

f = 1 Mc/s

I_m (amp)	0.5	0.6	0.7	0.8	
A_{100} (mm^2)	1.28	1.60	1.92	2.26	
A_{1k} (mm^2)	1.89	2.40	2.75	3.17	
A_{1k}/A_{100}	1.48	1.50	1.43	1.40	(1.45 av)
I_{av1k}/I_{av100}		Average	1.50		

f = 5 Mc/s

I_m (amp)	0.5	0.6	0.7	0.8	
A_{100} (mm^2)	1.10	1.48	1.70	1.95	
A_{1k} (mm^2)	1.34	1.80	2.16	2.40	
A_{1k}/A_{100}	1.22	1.22	1.27	1.23	(1.23 av)
I_{av1k}/I_{av100}		average	1.24		

In this table:

A_{100} = discharge area with R_s = 100 ohms

A_{1k} = discharge area with R_s = 1 kΩ

I_{av100} = average discharge current with R_s = 100 ohms

I_{av1k} = average discharge current with R_s = 1 kΩ

The average currents were determined from photographs of the corresponding current waveforms by integrating with a planimeter. They were only determined for I_m = 0.7 amps and assumed equal for the other currents, since the current waveforms do not change significantly between 0.5 and 0.8 amps.

These results show, that with a constant I_m, the discharge area varies as much as 50% at 1 Mc/s. An analysis of the waveforms, however, shows that the average current increases by the same factor (1.50) as the area. The measurements made at 5 Mc/s yields a similar result. This result suggests that the average current is more closely related to the area covered by the discharge than the peak current. However, the number of measurements made is not large enough to permit a firm statement about this point. The numerical value of the average current density J_{av} is ≈15 amp/cm^2. It is, however, very inconvenient to determine the average value of a waveform as distorted as the current waveform. Therefore the measurements of J made and shown in Figure 24 refer to the peak value of current, with a waveform corresponding to R_s = 500 ohms. For this waveform we get $I_{av} \approx 0.5\ I_m$, and $J_{av} \approx 0.5\ J_n$.

(c) Frequency

The discharge areas found for different frequencies are plotted in Figure 24. There seems to be a slight frequency effect such that the discharge area increases with frequency, when I_m = constant. This effect, however, may be caused by changes in the waveforms.

(d) Temperature and Electrode Shape

By "temperature" we will refer to the temperature of the electrode surface. The influence of this parameter can be demonstrated by the following experiment. We use a rod shaped electrode of 1 mm diameter. This diameter is small enough to make a 0.8 amp discharge cover not only the circular end face of the rod but also a considerable part of the cylinder surface. Thus we can measure the length of the discharge covered part of the rod accurately. First we will make the rod length ℓ_1 = 3.2 mm, then ℓ_2 = 1.8 mm. With these different lengths we will obtain different heat resistances along the rod and thus build up different temperatures at the rod end when maintaining discharges of equal power dissipation

For an estimation of what temperature to expect we assume that all the discharge power is delivered to the end face of the rod and that the other end of the rod is connected to a heat sink of constant temperature (cooling water). The temperature difference which will develop between the two rod ends can be calculated from.

$$\Delta T = \frac{Q\ell}{t \cdot A_r} ;$$

where $P = Q/t$ = Power delivered to rod

λ = heat conductivity of electrode material

ℓ = rod length

A_r = rod cross-section

For copper we find $\lambda = 0.9$ cal/cm sec °C (reference 7)

For a 0.8 amp discharge (P = 120 watts, section IV, f) 60 watts would be delivered to each electrode. This gives $Q/t = 15$ cal/sec. $\ell = 0.32$ cm and $A_r = 0.78 \cdot 10^{-2}$ cm² (1 mm rod diameter). From this we obtain $\Delta T = 680°$ C. This estimate is certainly too high, because first, not all heat dissipated in the discharge is delivered to the electrodes (some of it is used to heat the surrounding air); second, not all the heat delivered to the electrode is traveling through the entire length ℓ. Some of it enters closer to the cool end, which reduces the temperature built up at the hot end of the rod. But we can still say that the electrode surface temperature will be in the order of several hundred degrees centigrade, which is significantly different from the temperature of a well cooled electrode (a plane parallel electrode of 3.2 mm diameter yields $\Delta T = 75°$ C). The temperature difference can be seen under the microscope, since the rod electrodes became red hot. For a rod length of 0.18 cm the same consideration would result in $\Delta T = 380°$ C. The results of measurements of discharge areas for these two electrodes are plotted in Figure 25. Higher temperature of electrode surface results in more area covered by the discharge. The electrode shape as such seems to have no influence on current density. Only by a secondary effect, inasmuch as different shapes may result in different surface temperatures, will different J be obtained. For example, four different electrode shapes yield the following discharge areas:

plane parallel	2.4 mm²	
cone	2.4 mm²	All for $I_m = 0.8$A
long rod, $\ell_1 = 3.2$ mm	4.95 mm²	at f = 5 Mc/s
short rod, $\ell_2 = 1.8$ mm	3.30 mm²	

(e) Electrode Distance and Materials

Within the accuracy of measurement the current density was found to be independent of the electrode distance.

Measurements with respect to the influence of material were only made on copper and brass. No difference in current density was found.

f. Power Dissipated in Discharge

With the instantaneous values of discharge current i and voltage v, the power dissipated in the discharge is:

$$P = 1/T \int_0^T iv \, dt$$

The power can be calculated from the waveforms given in the Figures 8-11.

Some of this power will heat the air around the discharge, most of it will heat the electrodes by ion impact. Here we are only considering the total power as given by the above expression. Obviously, since the waveforms depend on R_s, frequency, etc. so does the power. Therefore we will only give an order of magnitude by considering two cases:

(1) f = 1 Mc/s, R_s = 500 ohms, d = 0.05 mm

(2) f = 5 Mc/s, R_s = 500 ohms, d = 1 mm

With these quantities we find power as a function of peak current. The result is plotted in Figure 26. For other parameters the power can be obtained by considering the influence of the parameters as discussed earlier in this report.

It should be noted that discharge power does not increase with the square of the current, since voltage is almost a constant. It is not a completely linear relationship either , however, because some change in waveform is involved when changing I_m. The highest current measured was 2 amps, this being the limit of the power generator. At this level of 2 amps a stable glow discharge can be maintained between cooled copper electrodes. (See Figure 21 (c)).

There is a minimum power necessary to maintain a discharge. This minimum seems to be approximately 5 watts. With R_s = 500 ohms a discharge with I_m = 0.1 amp and P = 8 watts can be maintained. An I_m less than 0.1 amp is difficult to establish with R_s = 500 ohms. The discharge has a tendency to stop. Still lower current can be obtained with larger values of R_s. With R_s = 10 kΩ, for example, I_m = 50 milliamps can be maintained. The power dissipated in this discharge is approximately 4 watts. Below this power level no discharge could be maintained. So, under the conditions described in this report, I_m = 50 milliamps and P = 4 watts seem to be the minimum values necessary to maintain an rf glow discharge.

V. CONCLUSIONS

We have investigated rf glow discharges in air at atmospheric pressure, in the frequency range 1-25 Mc/s.

From typical waveforms of current and voltage, it can be concluded that ignition and extinction take place in every halfcycle. The waveforms depend not only on discharge properties, but also on the electric circuit associated with the discharge. With the exception of I_c (Figure 2), the waveforms seem to be independent of frequency when operated with constant associated circuit impedances.

A minimum voltage is required to maintain the discharges. At the smallest adjustable electrode distances this minimum voltage is 270 volts.

The voltage V_m necessary to maintain the discharge is essentially independent of all parameters except the electrode distance d. The rate of change of V_m with d depends on d and was found to be between 500 V/cm and 10,000 V/cm. All other parameters change V_m by only small amounts ($\approx$ 10%) in the ranges investigated.

The current range examined was 50 milliamps to 2 amps peak current. Below I_m = 50 milliamps no discharge could be maintained; the upper limit of 2 amps was set by limitations of the available equipment. The associated power levels are 4 watts minimum power necessary to maintain a discharge, and 300 watts maximum discharge power, limited by the equipment capabilities.

Within the current range examined the electrode area covered by the discharge is proportional to the current. The current density is constant as a function of I_m. As a first order approximation the current density is independent of all other parameters.

The essential discharge properties of rf and dc glow discharges are summarized in the following table:

	rf discharges	dc glow discharges
appearance	symmetrical	asymmetrical
minimum voltage (d≈0.02mm)	270 volts	275 volts

Current density	J_{av} = 15 amp/cm^2	J = 10-15 amp/cm^2 (reference 4)
Difference of V for different materials (Ni, Fe, Cu, Au)	<10%	<10%

Important features of rf discharges equal or approximate those of dc glow discharges. Furthermore, Fletcher (reference 8) has shown that breakdown in air at atmospheric pressure can take place within times shorter than 1 ns. One half cycle even at the highest frequency investigated (25 Mc/s) still lasts 20 ns, thus there is ample time in each half cycle to establish, maintain and extinguish the discharge. Breakdown in such short times can of course only occur if a sufficiently large number of electrons is available at the cathode at the time of breakdown initiation.

There are several mechanisms possible in an rf discharge which could provide such electrons: photoemission or secondary emission by positive ion impact or by impact of molecules in a metastable state. These mechanisms are possible because ionization and/or excitation of the discharge gas are maintained to a certain extent during the time between extinction of the discharge after the previous half cycle and reiginition in the new half cycle. If this were not so, (for example if all ionization were lost by recombination and all molecules returned to the ground state) the discharge could not continue. Therefore a voltage which is large enough to maintain a discharge is not large enough to cause breakdown of a gap from a "no discharge" condition. To initially establish a discharge, the electrodes must therefore be touched together and pulled apart.

REFERENCES

(1) Lysher, L. J. "An Investigation of HERO Problems Involving RF Arcs and Some Proposals for Their Solutions." NWL, Dahlgren, Technical Memorandum No. W-1/64

(2) Schwab, H. A. "The Present State of the NWL RF Discharge Investigation." NWL, Dahlgren, Technical Memorandum No. W-20/65

(3) Haworth, "Electrode Reactions in the Glow Discharge" Journal of Applied Physics Volume 22, May 1951, page 606

(4) Gambling-Edels, "The High Pressure Glow Discharge in Air", Brit. Journ. of Appl. Phys. 5, 36, 1954

(5) Francis, "The Glow Discharge at Low Pressure", Encyclopedia of Physics, edited by S. Fluegge, 1956, Volume XXII

(6) Brown, S. C., "Basic Data of Plasma Physics", John Wiley & Sons, New York 1959

(7) Handbook of Chemistry and Physics, Chemical Rubber Publishing Company, Cleveland, Ohio 37th ed, 1955/56

(8) Fletcher, "Impulse Breakdown in the 10^{-9} sec range of Air at Atmospheric Pressure", Phys. Rev. Vol 76, No. 10, Nov 1949, page 1501.

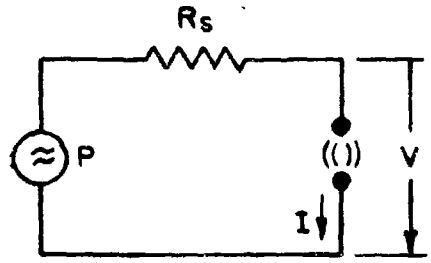

FIGURE 1 DISCHARGE CIRCUIT

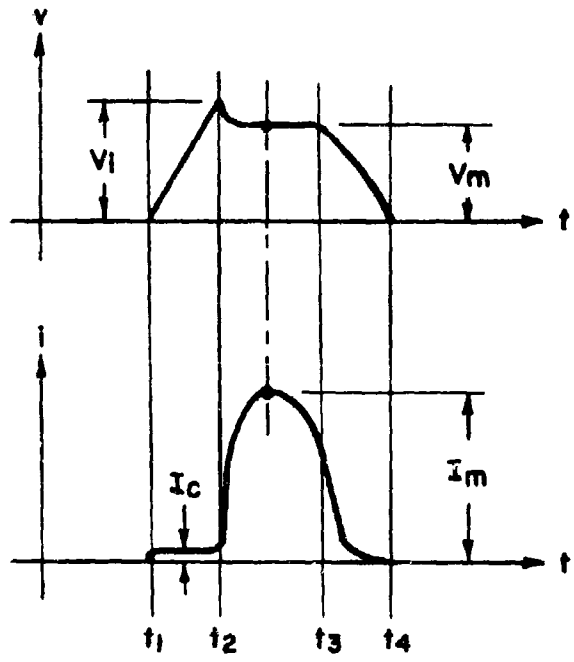

FIGURE 2 VOLTAGE AND CURRENT IN ONE HALFCYCLE

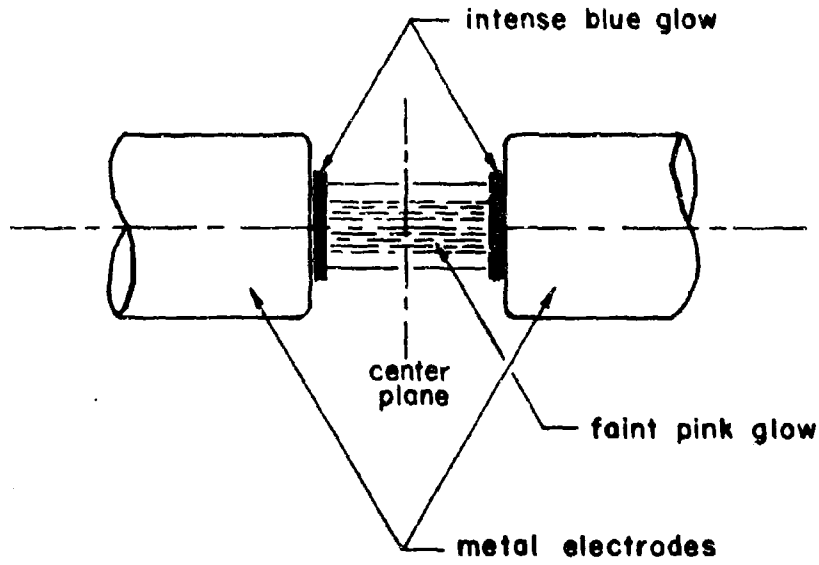

(a)

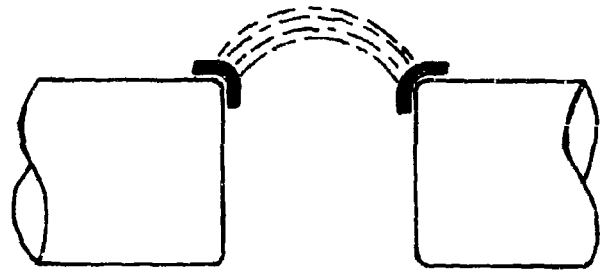

(b)

FIGURE 3 APPEARANCE OF DISCHARGE

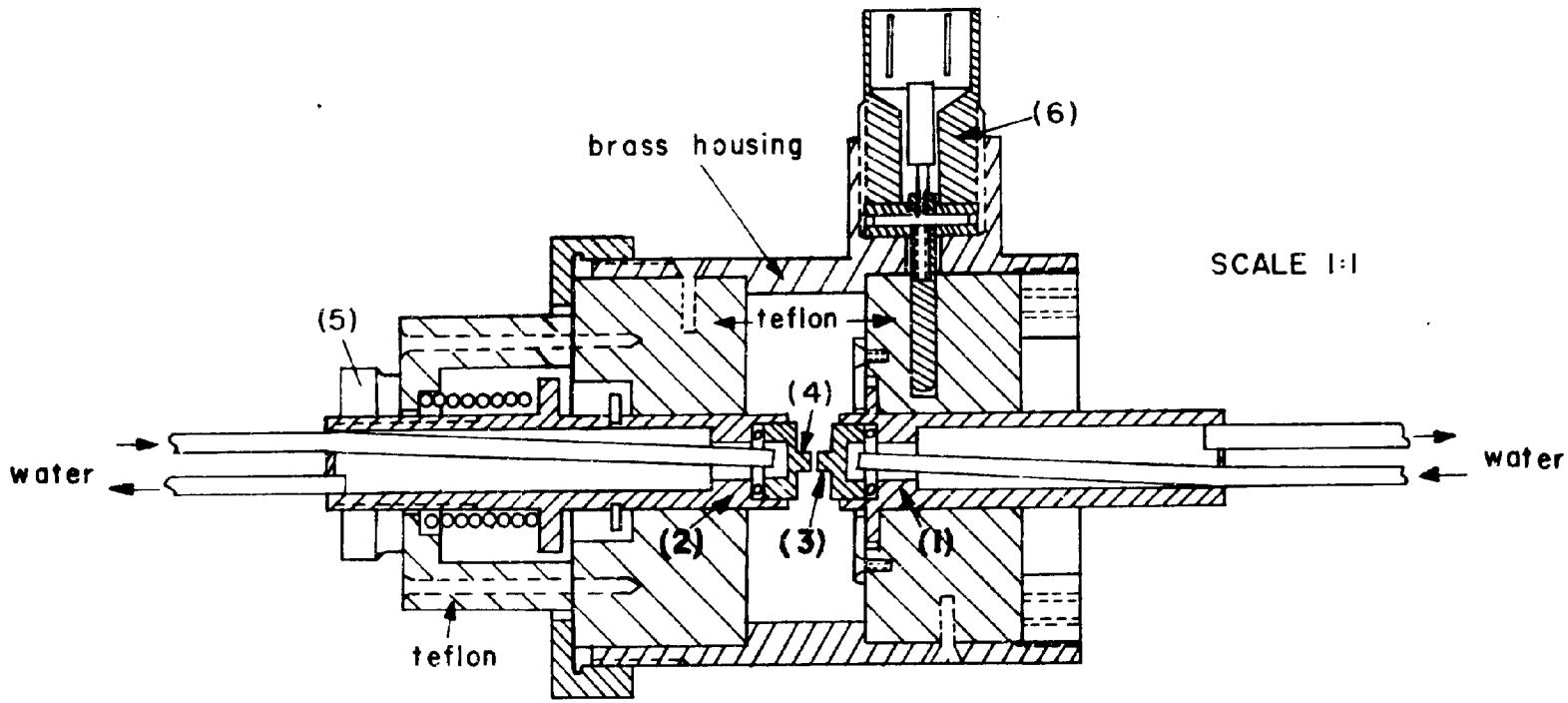

FIGURE 4 ELECTRODE ASSEMBLY

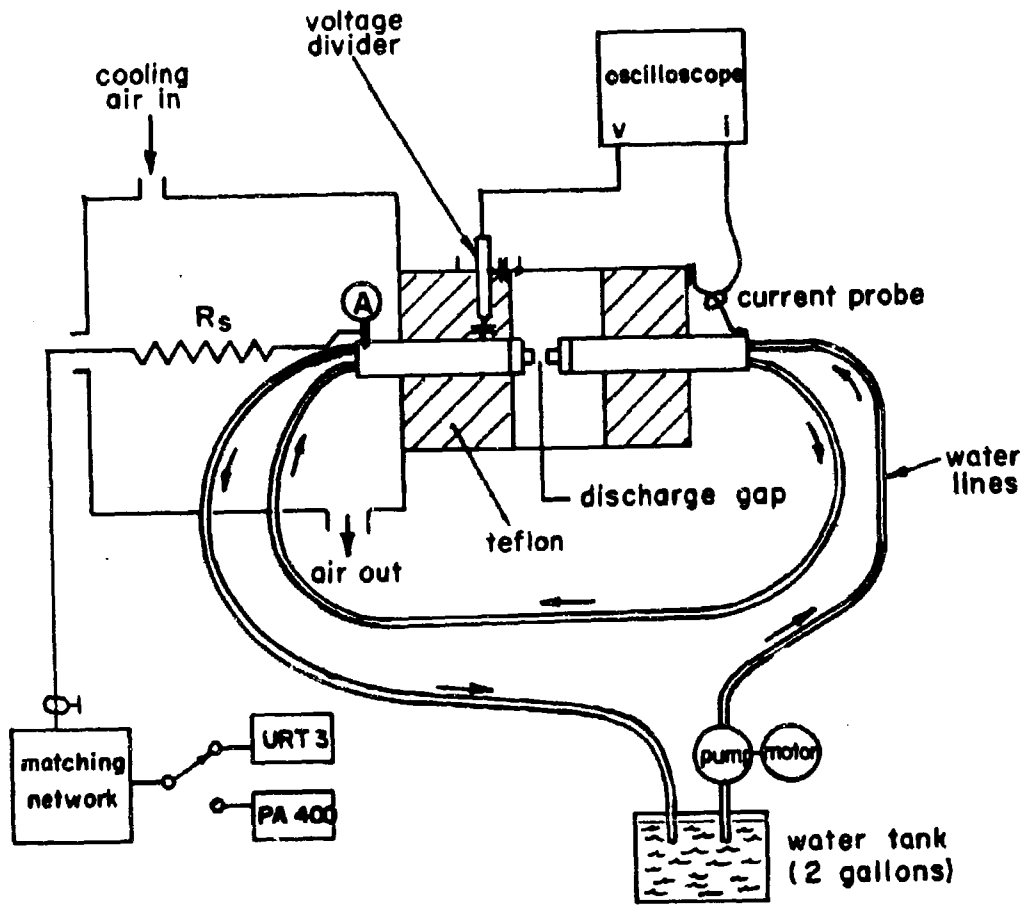

FIGURE 5 SYSTEM BLOCK DIAGRAM

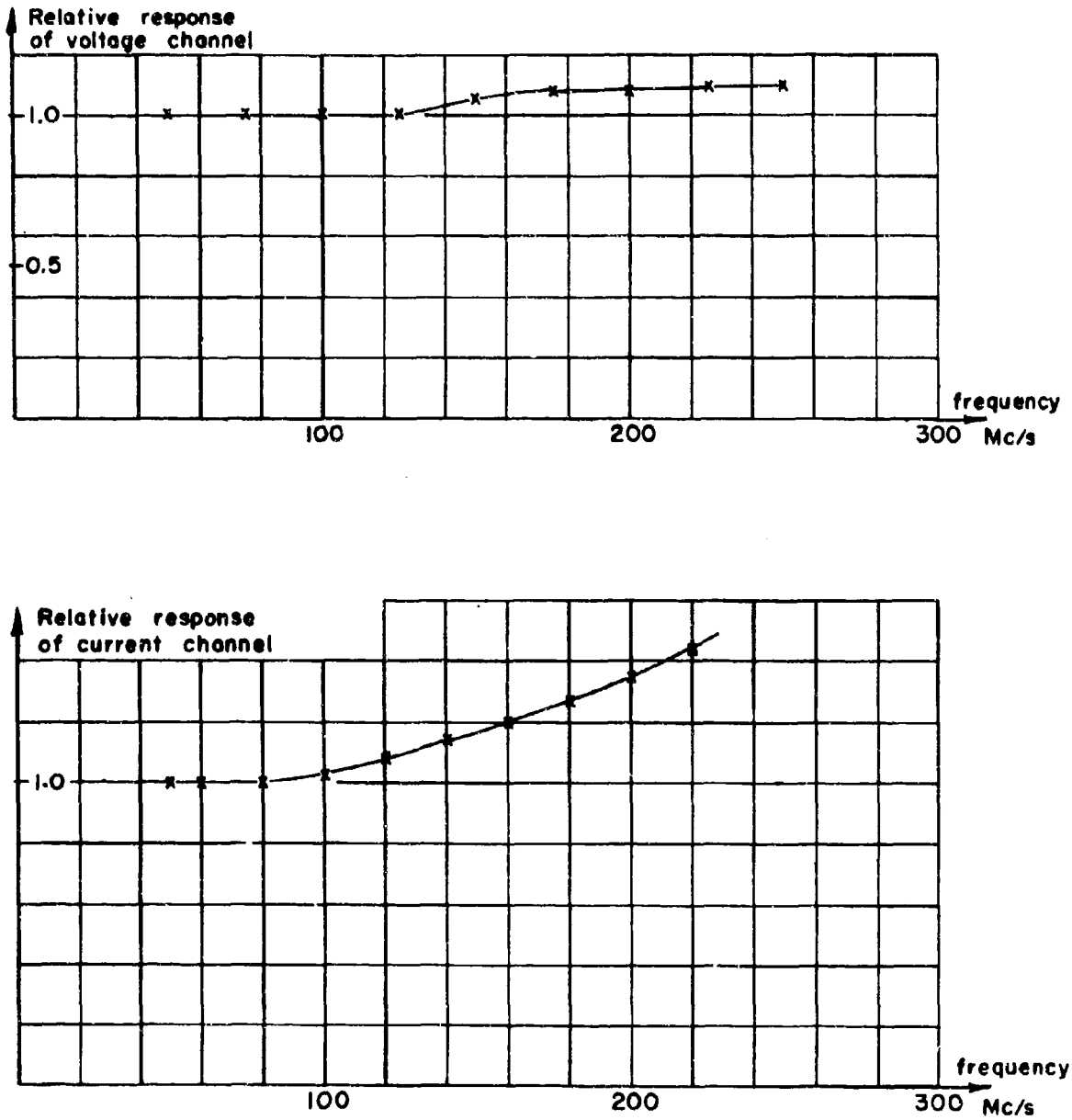

FIGURE 6 FREQUENCY RESPONSE OF MEASURING SYSTEM

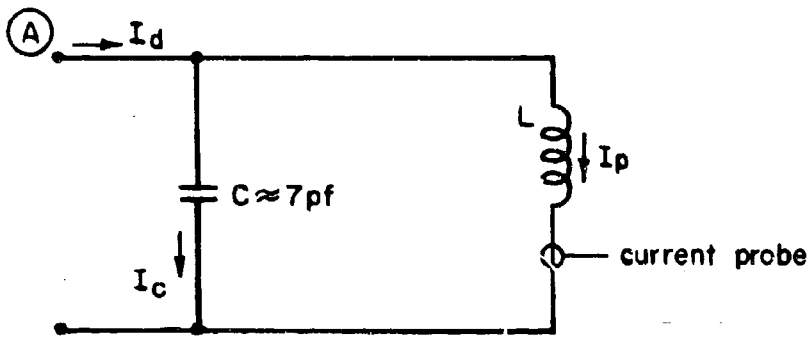

FIGURE 7 CIRCUIT ASSOCIATED WITH CURRENT PROBE

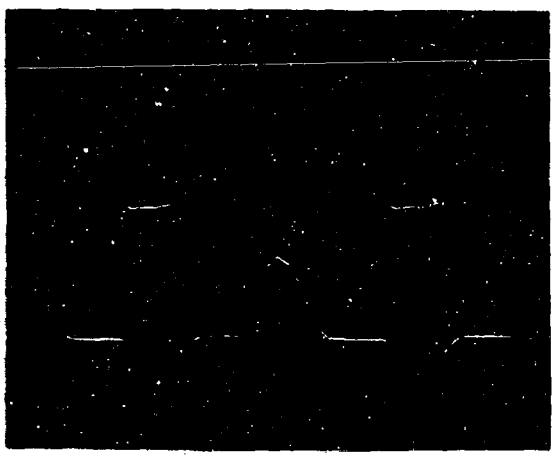

(a) $d = 2d_o$ $0.2 \frac{amp}{div}$

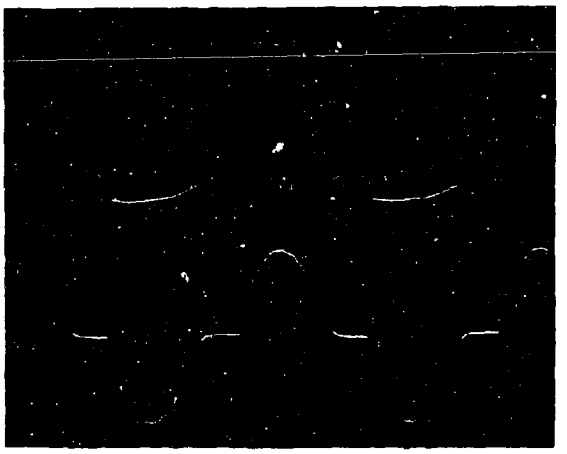

(b) $d = 2d_o$ $0.5 \frac{amp}{div}$

(c) $d = 8d_o$ $0.2 \frac{amp}{div}$

(d) $d = 10d_o$ $0.5 \frac{amp}{div}$

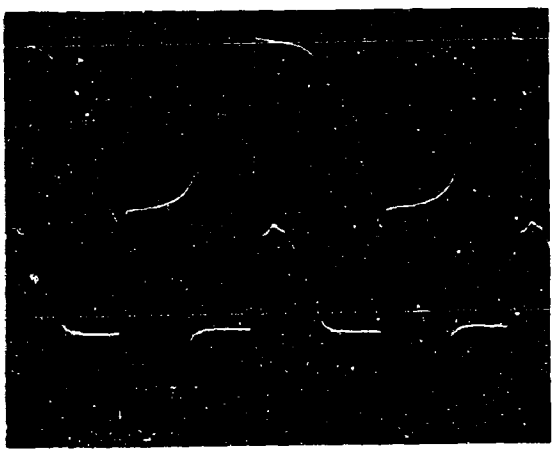

(e) $d = 2.5d_o$ $0.2 \frac{amp}{div}$

Upper waveform: voltage, $200 \frac{volts}{div}$

Lower waveform: current

$R_S = 500$

FIGURE 8 WAVEFORMS AT 1 Mc/s

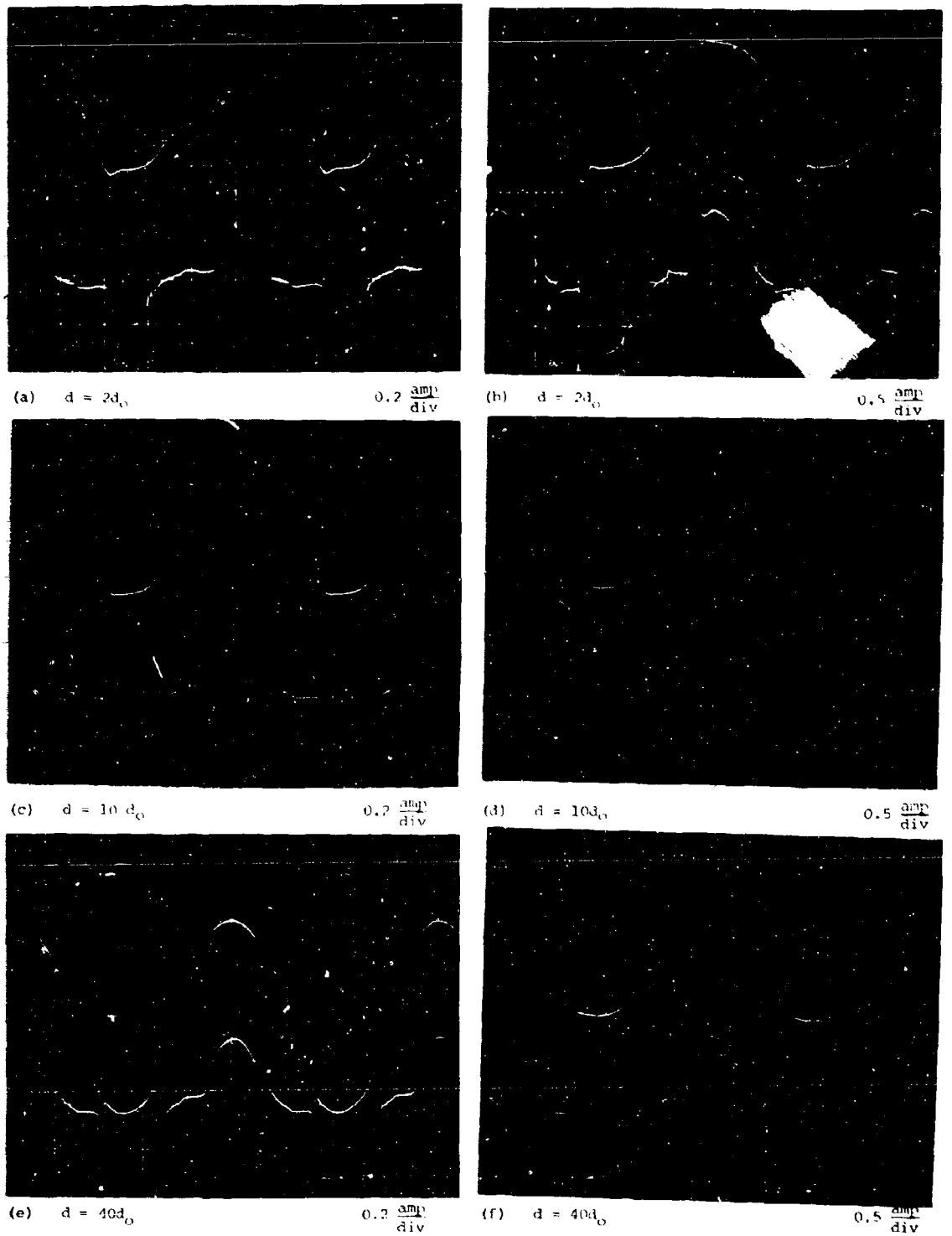

(a) $d = 2d_o$ $0.2 \frac{amp}{div}$ (b) $d = 2d_o$ $0.5 \frac{amp}{div}$

(c) $d = 10\ d_o$ $0.2 \frac{amp}{div}$ (d) $d = 10d_o$ $0.5 \frac{amp}{div}$

(e) $d = 40d_o$ $0.2 \frac{amp}{div}$ (f) $d = 40d_o$ $0.5 \frac{amp}{div}$

FIGURE 9 WAVEFORMS AT 5 Mc/s, $R_S = 500\Omega$

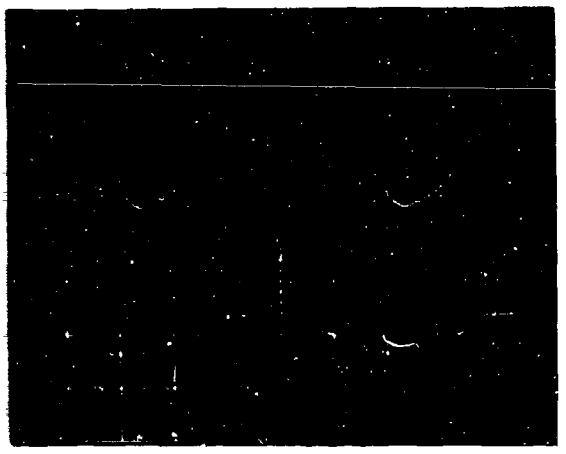

(a) $d = 2d_o$ $0.2 \frac{amp}{div}$

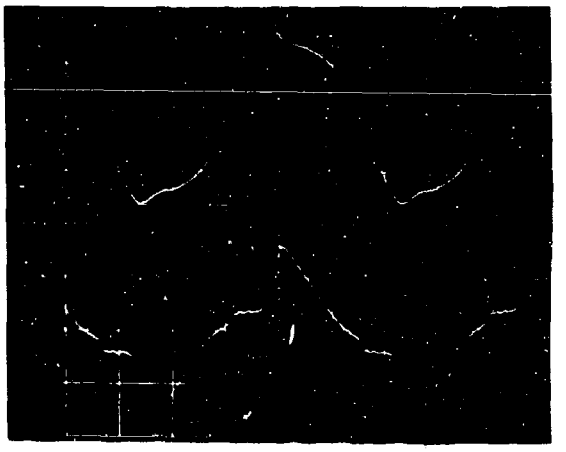

(b) $d = 2d_o$ $0.5 \frac{amp}{div}$

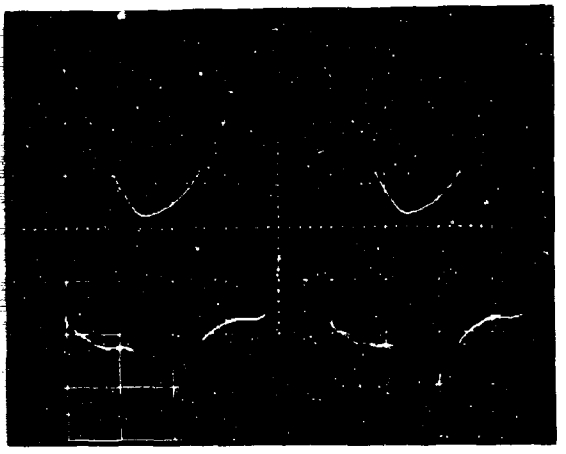

(c) $d = 10d_o$ $0.2 \frac{amp}{div}$

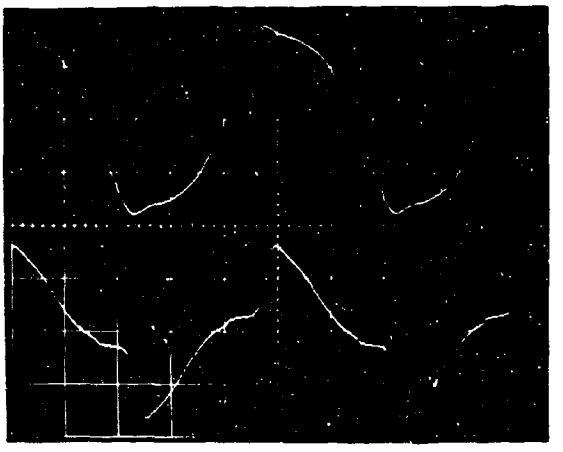

(d) $d = 10d_o$ $0.5 \frac{amp}{div}$

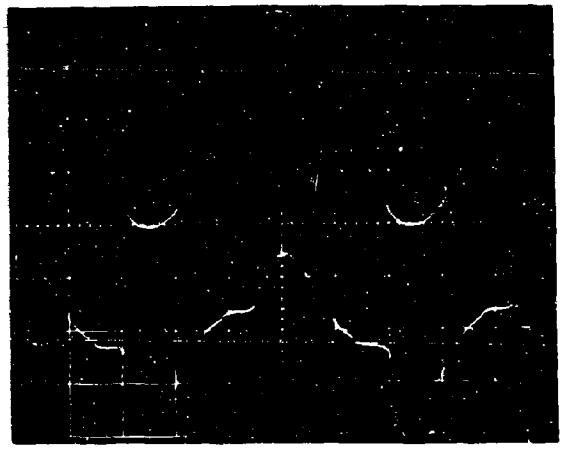

(e) $d = 40d_o$ $0.2 \frac{amp}{div}$

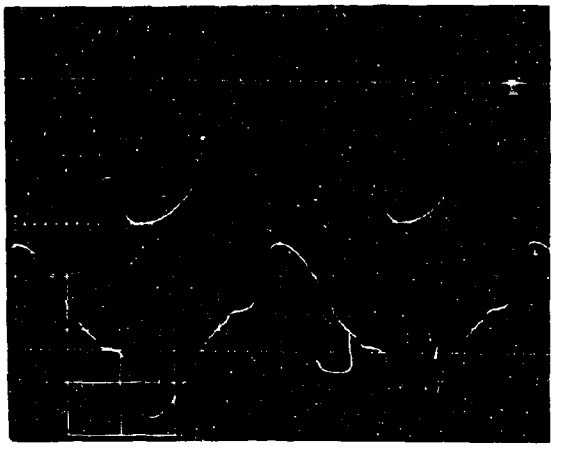

(f) $d = 40d_o$ $0.5 \frac{amp}{div}$

FIGURE 10 WAVEFORMS AT 10 Mc/s, $R_s = 500\Omega$

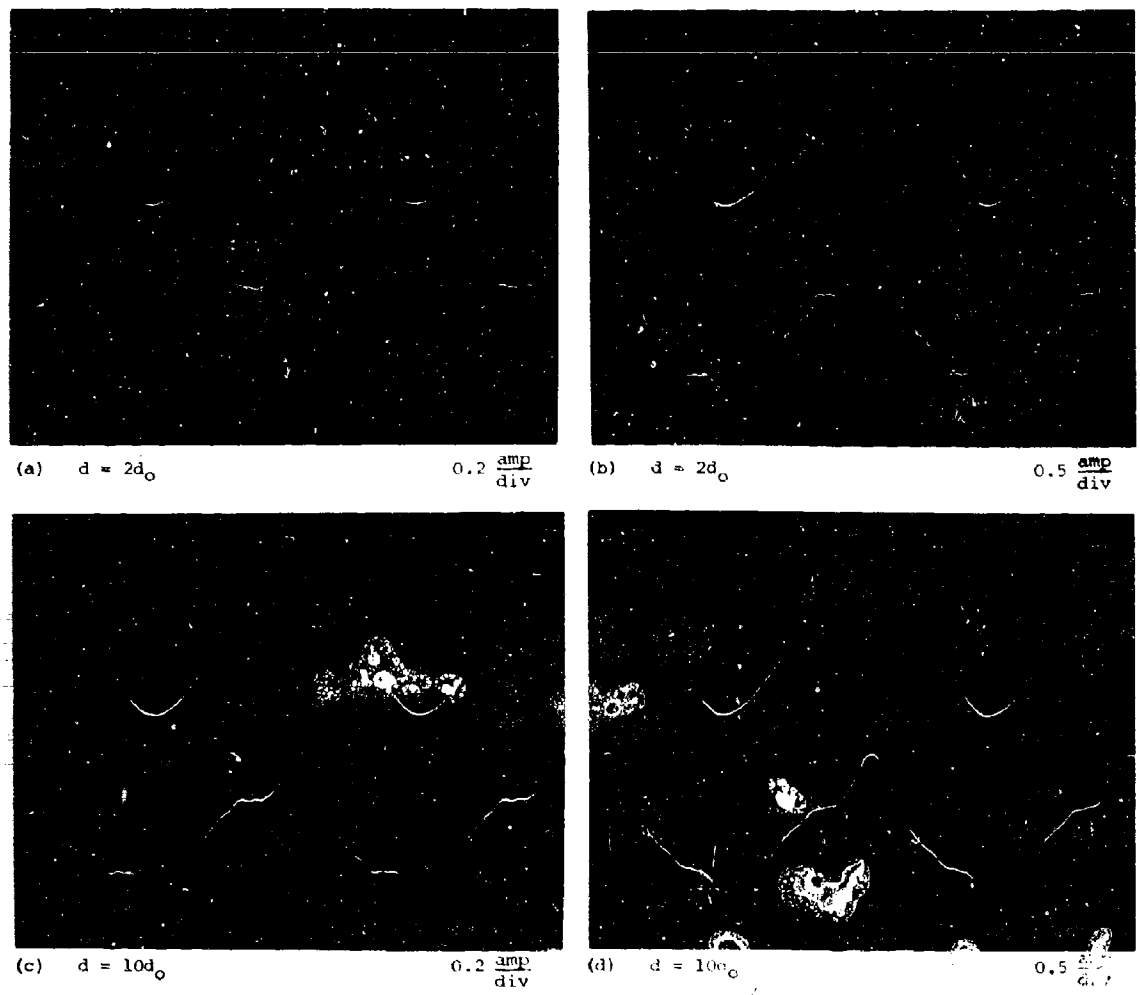

(a) $d = 2d_o$ 0.2 $\frac{amp}{div}$ (b) $d = 2d_o$ 0.5 $\frac{amp}{div}$

(c) $d = 10d_o$ 0.2 $\frac{amp}{div}$ (d) $d = 10d_o$ 0.5 $\frac{amp}{div}$

FIGURE 11 WAVEFORMS AT 25 Mc/s, $R_s = 37\Omega$

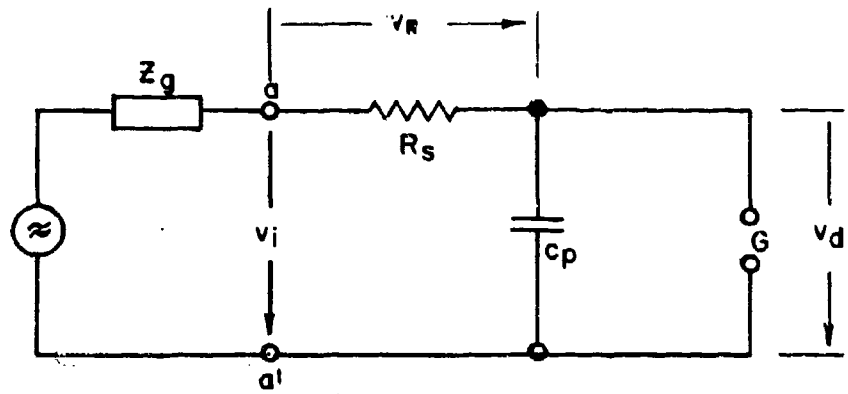

FIGURE 12 CIRCUIT ELEMENTS

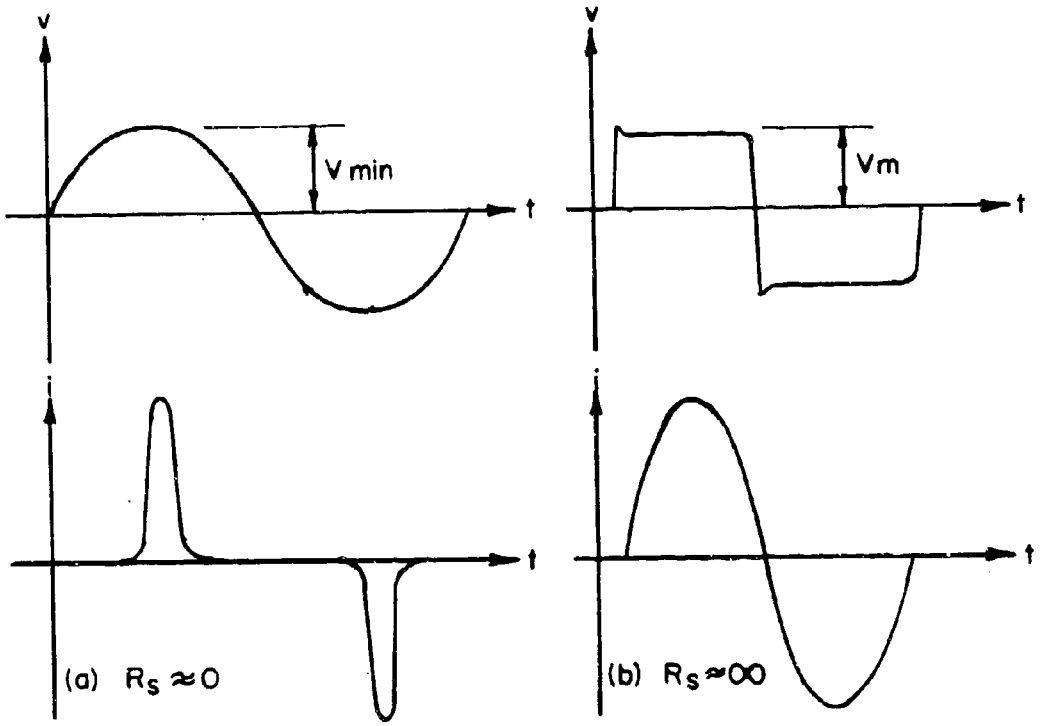

FIGURE 13 INFLUENCE OF R_S UPON WAVEFORM

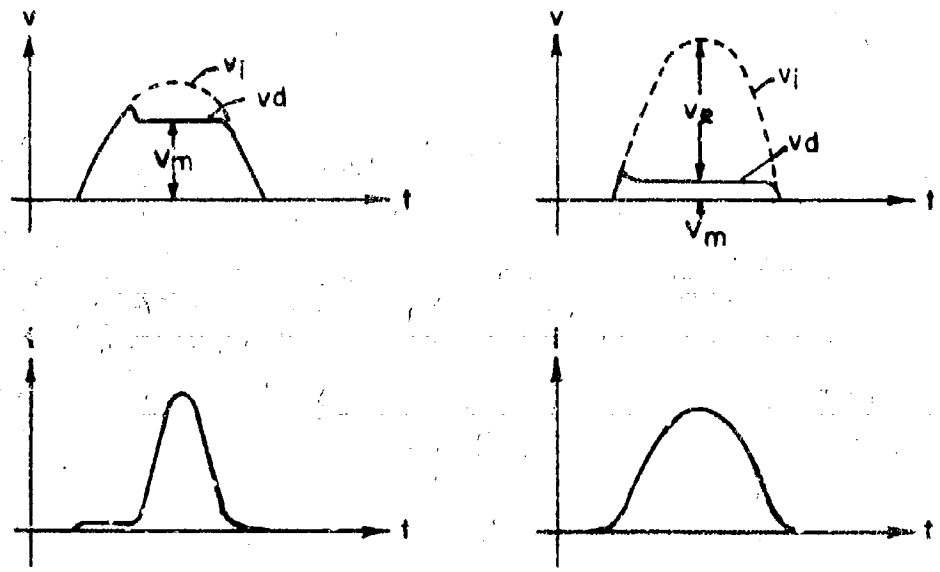

FIGURE 14

DIVISION OF INPUT VOLTAGE v_i BETWEEN DISCHARGE AND R_s

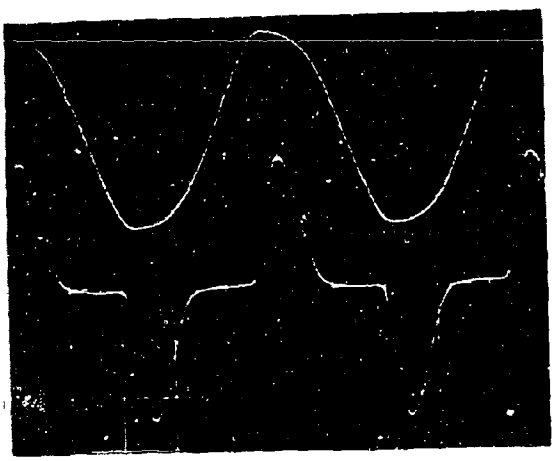

(a) R_S = 100. 1 Mc/s

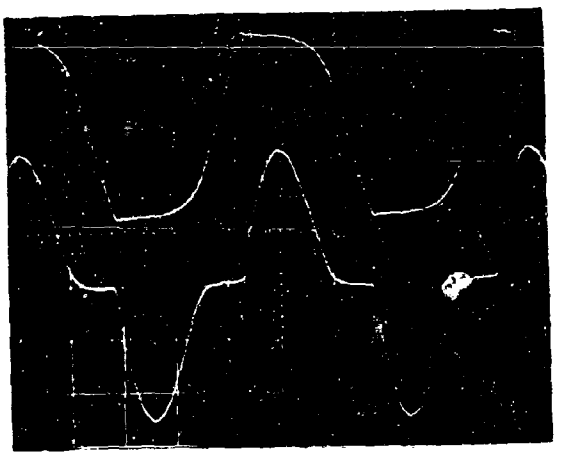

(b) R_S = 50. 1 Mc/s

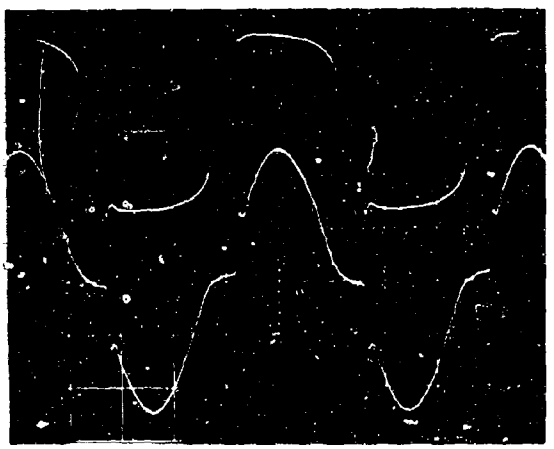

(c) R_S = 2000. 1 Mc/s

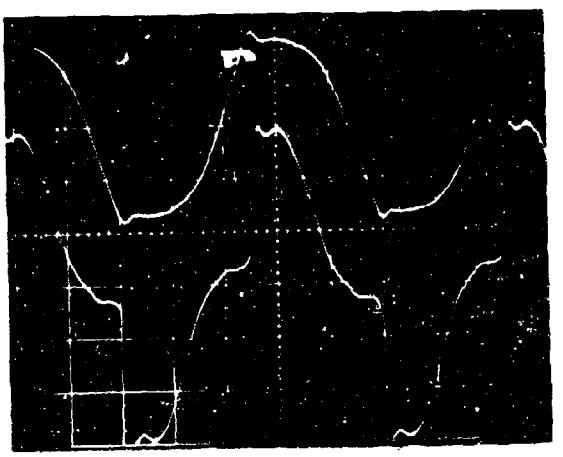

(d) C_D = 25 pF, R_S = 500. 5 Mc/s

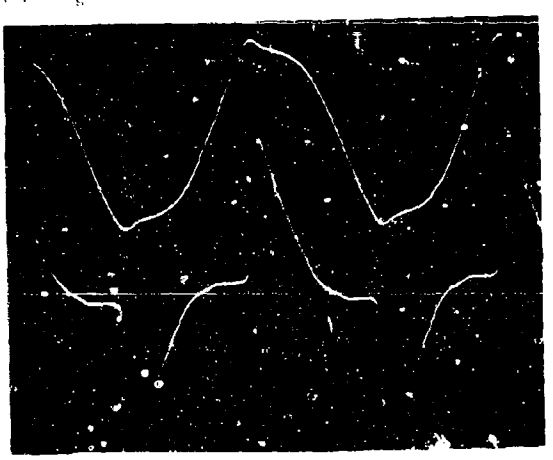

(e) C_D = 40 pF, R_S = 500. 5 Mc/s

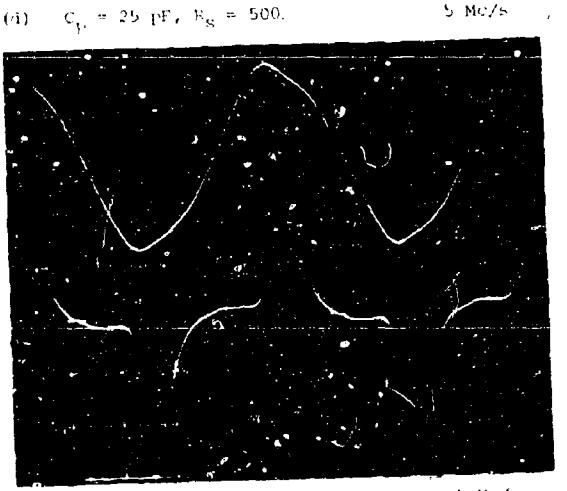

(f) C_D = 95 pF, R_S = 500. 5 Mc/s

All photographs: 2.00 $\frac{\text{volt}}{\text{div}}$, 0.2 $\frac{\mu\text{s}}{\text{div}}$, A = 5.

FIGURE 4. WAVEFORMS WITH VARIOUS R_S AND C_D

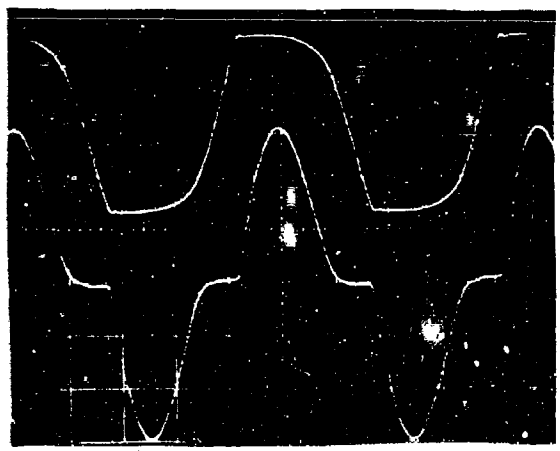

(a) C_p = 25 pF

(b) C_p = 75 pF

(c) C_p = 125 pF

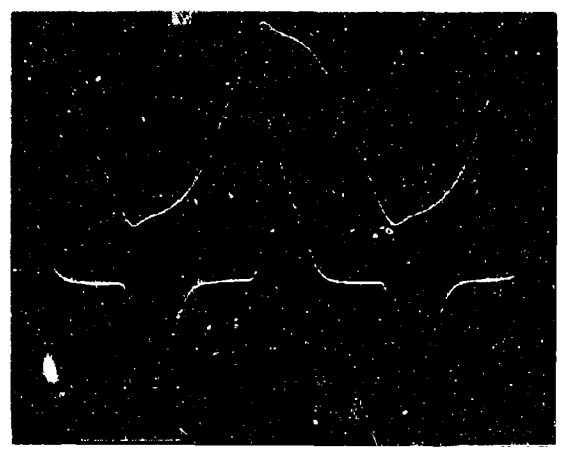

(d) C_p = 225 pF

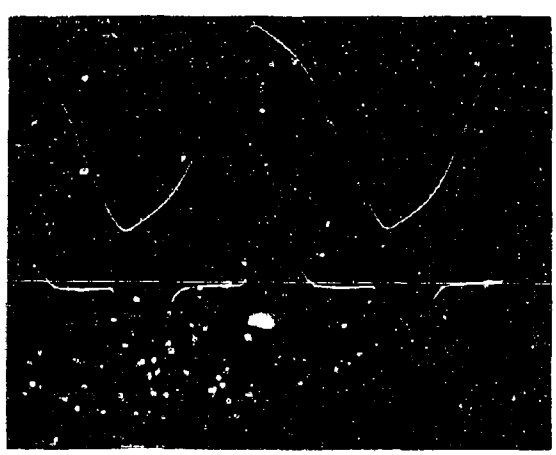

(e) C_p = 425 pF

f = 1 Mc/s

d - $5d_0$; 200 $\frac{\text{volts}}{\text{div}}$; 0.2 $\frac{\text{amp}}{\text{div}}$; K_s = 500.

FIGURE 16

INFLUENCE OF C_p ON DISCHARGE WAVEFORMS

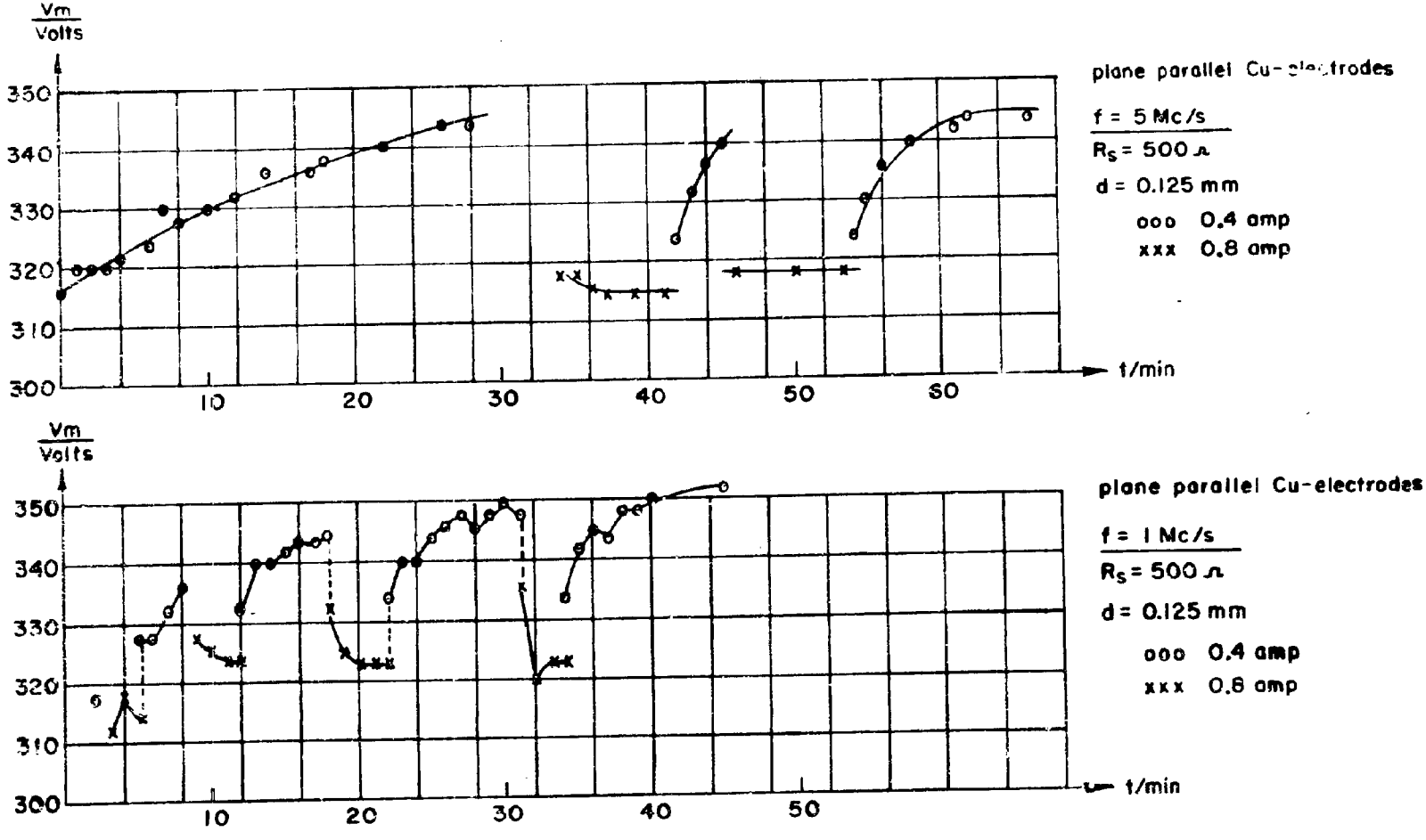

FIGURE 17 TIME DEPENDENCE OF V_m

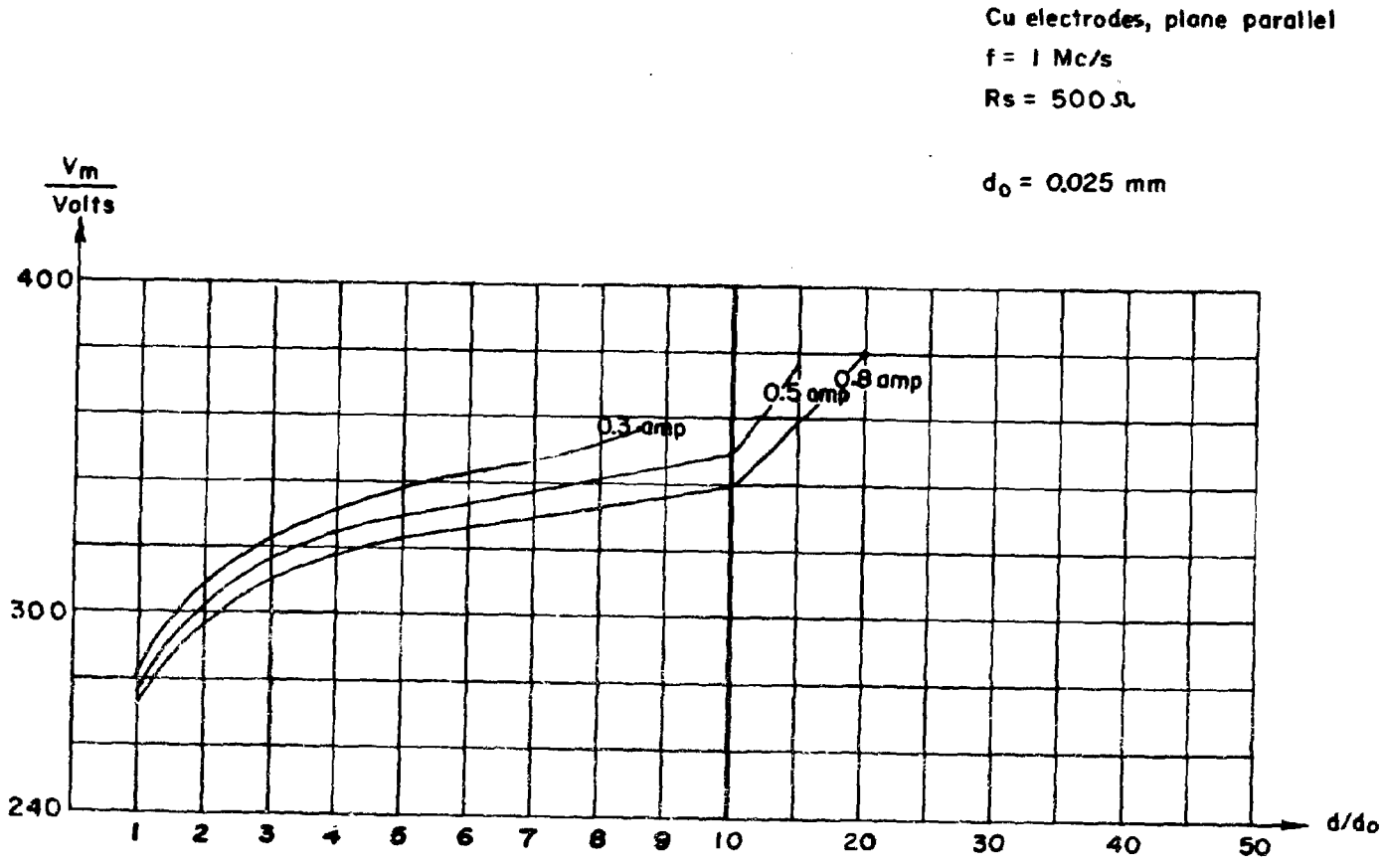

FIGURE 18 VARIATION OF V_m WITH d AT 1 Mc/s

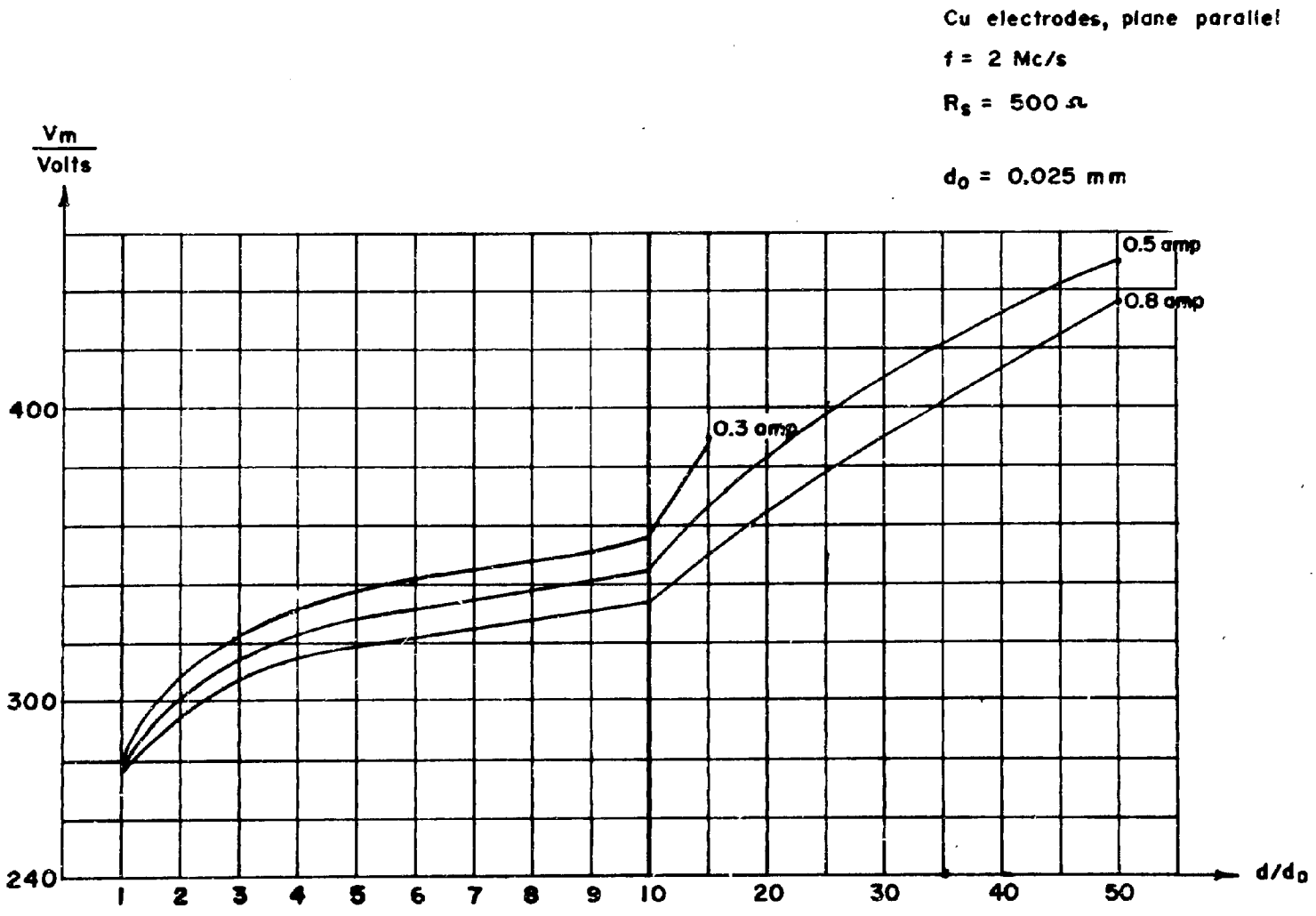

FIGURE 19 VARIATION OF V_m WITH d AT 2 Mc/s

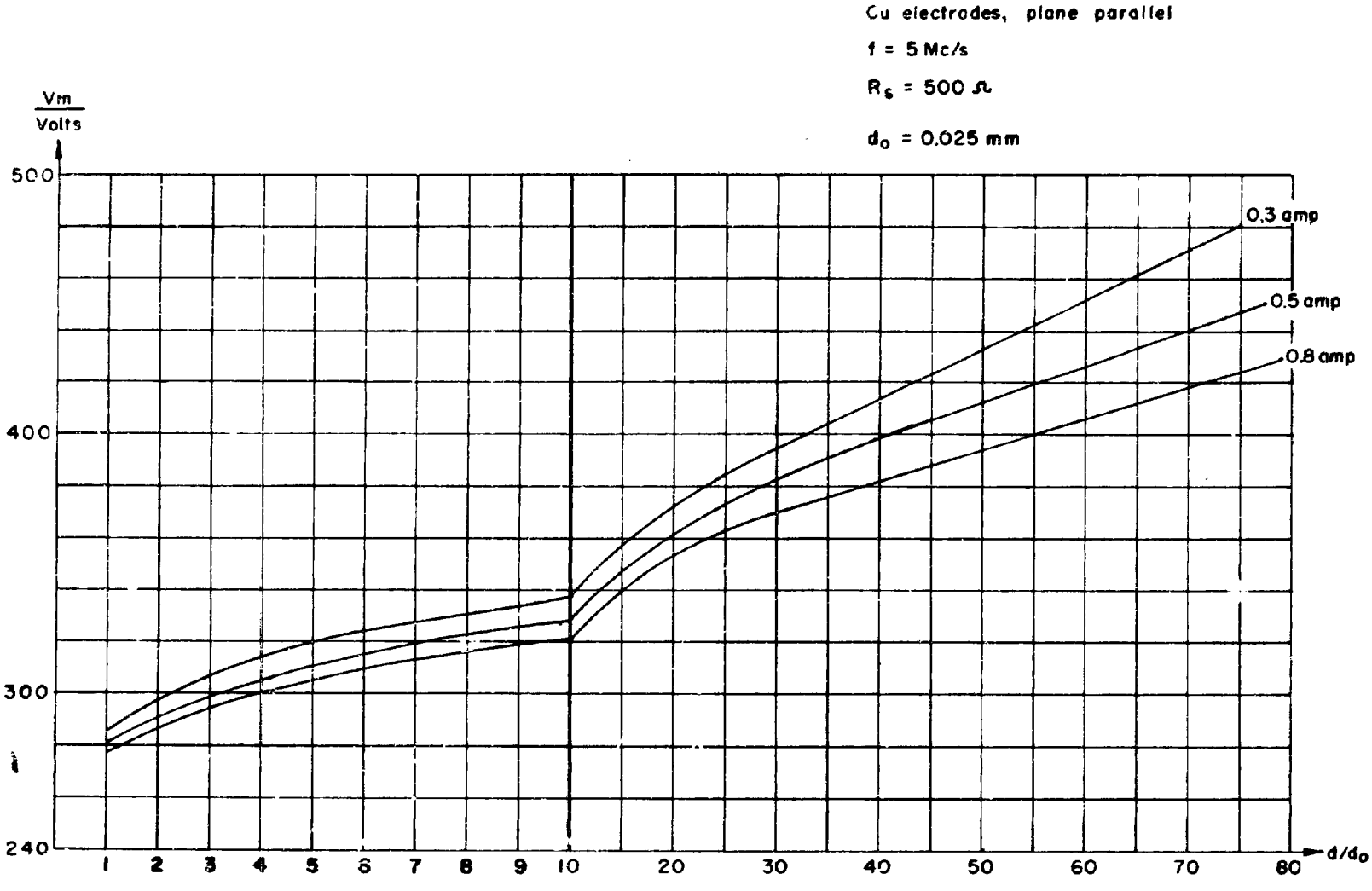

FIGURE 20 VARIATION OF V_m WITH d AT 5 Mc/s

(a)

(b)

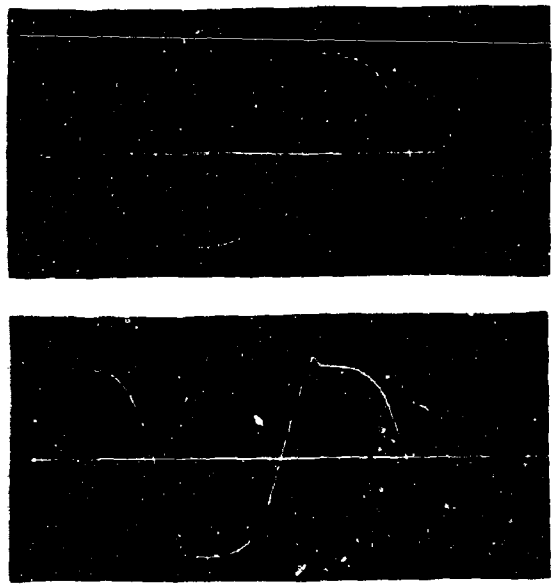

f = 1 Mc/s; d = $4d_0$;

200 $\frac{\text{volts}}{\text{div}}$; I_D = 0.4 amp ; R_S = 500Ω

FIGURE 21 (a) and (b) VOLTAGE ACROSS DISCHARGE BETWEEN TWO ELECTRODES OF DIFFERENT MATERIAL (Al AND Cu)

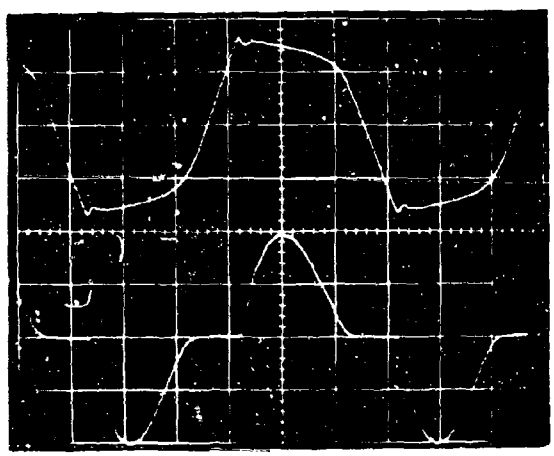

FIGURE 21 (c) 2 AMPERE-DISCHARGE

d = $3d_0$; 1 Mc/s; 200 $\frac{\text{volts}}{\text{div}}$; 1.0 $\frac{\text{amp}}{\text{div}}$; R_S = 100Ω

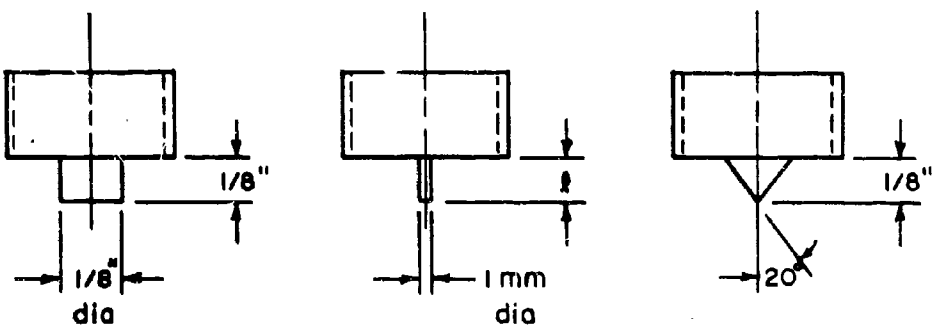

(a) plane parallel electrode

(b) rod electrode

(c) cone electrode

FIGURE 22 DIFFERENT ELECTRODE SHAPES

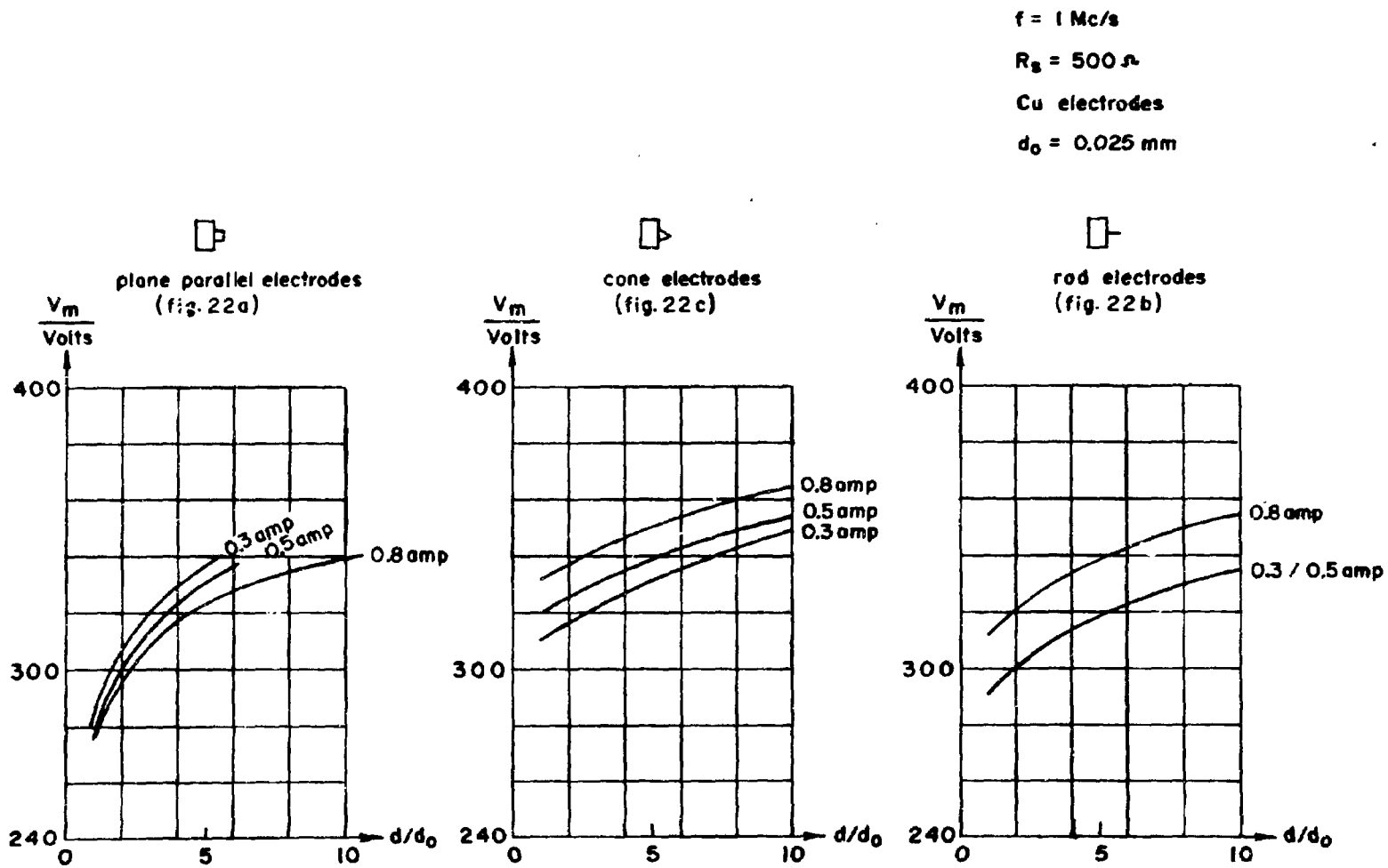

FIGURE 23 VARIATION OF V_m WITH ELECTRODE SHAPE

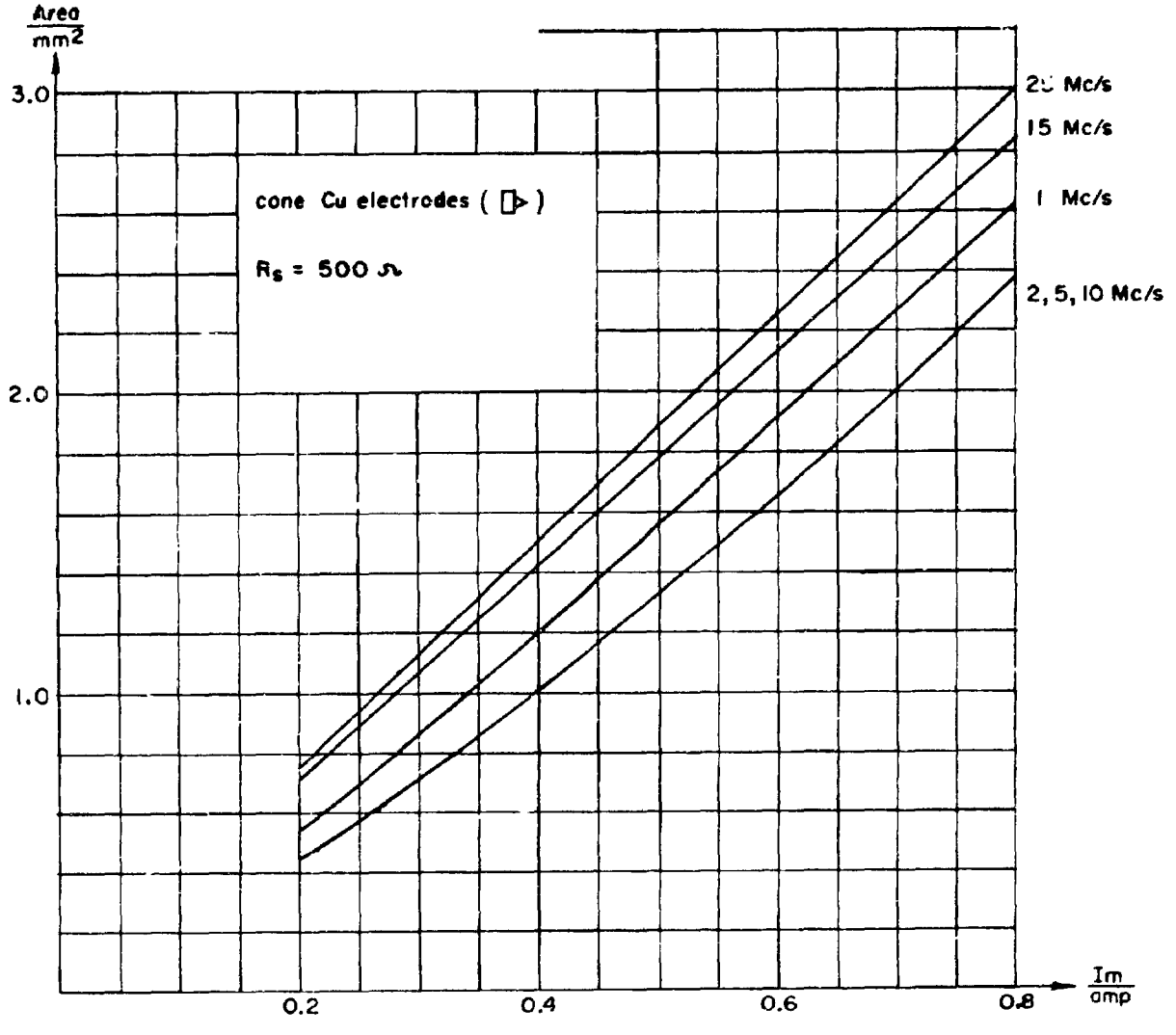

FIGURE 24 AREA COVERED BY THE DISCHARGE

Cu – electrodes

$R_s = 500\,\Omega$

5 Mc/s

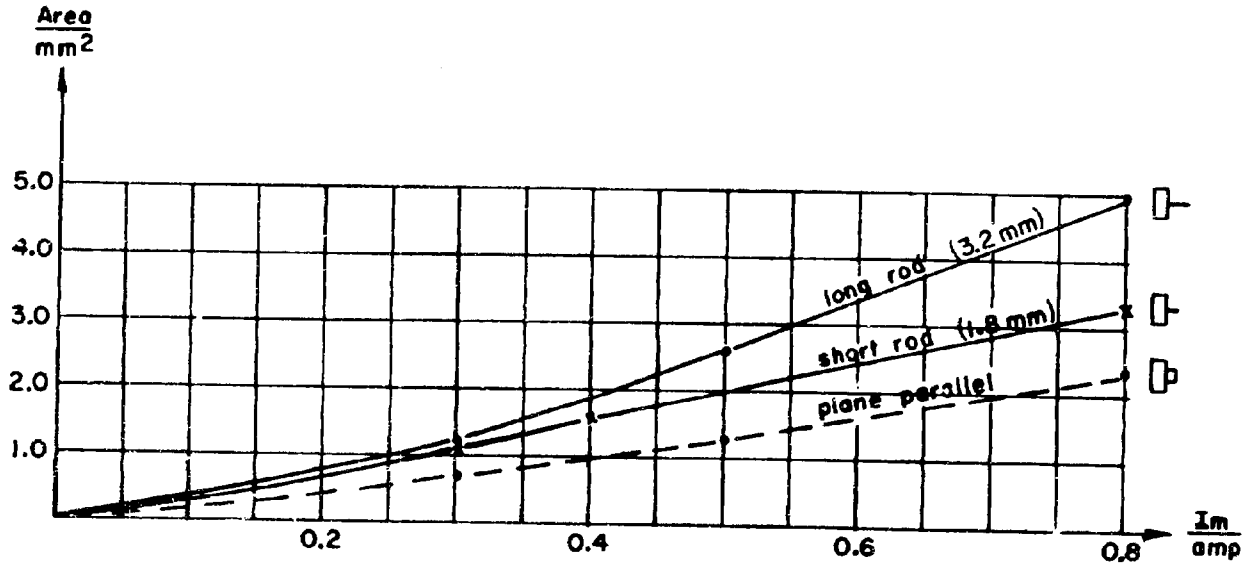

FIGURE 25 VARIATION OF DISCHARGE AREA WITH ELECTRODE SHAPE

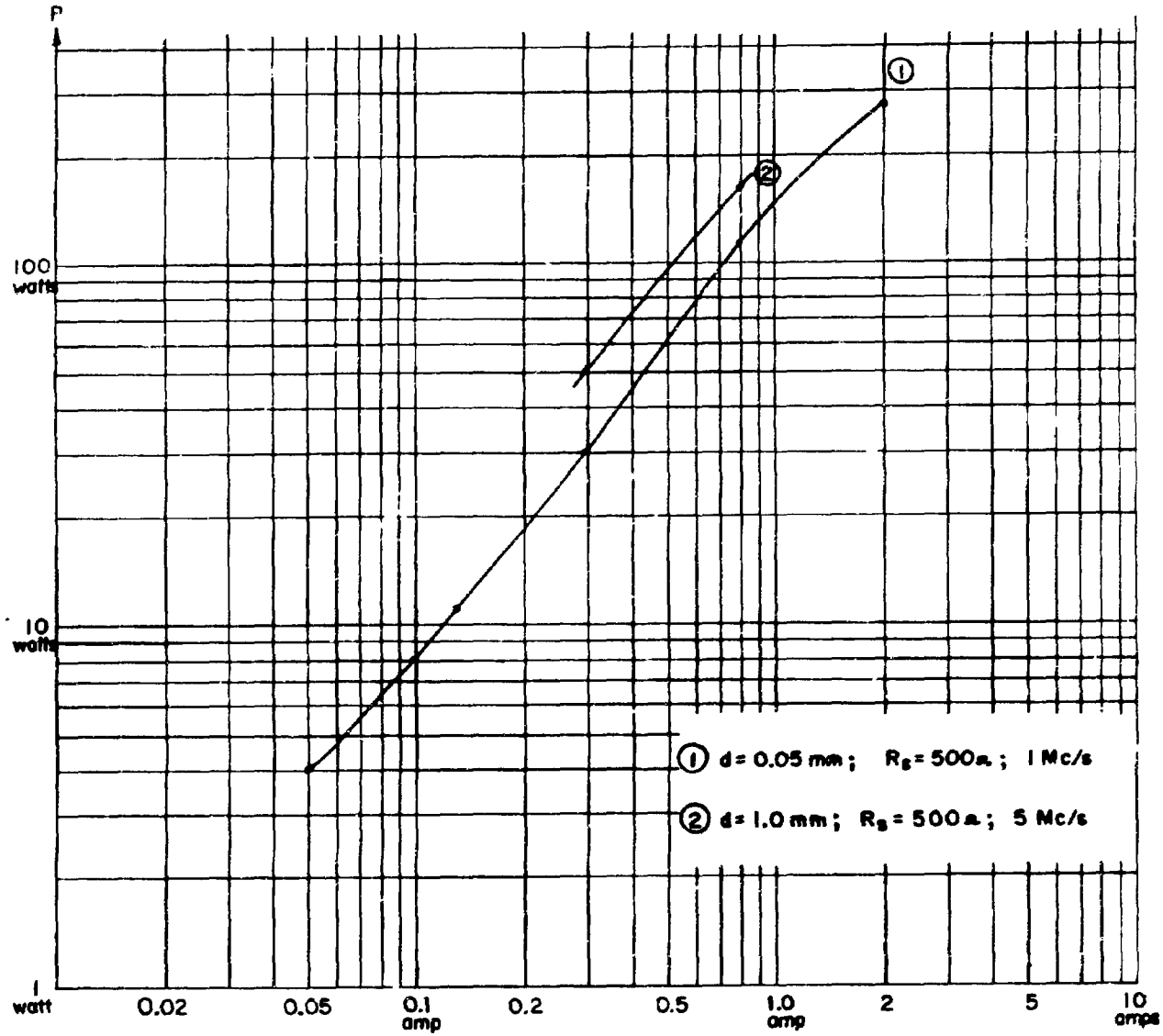

FIGURE 26 POWER DISSIPATED IN DISCHARGE

APPENDIX A

DC GLOW DISCHARGE QUANTITIES AT ATMOSPHERIC PRESSURE

There are reports on dc glow discharges in air at atmospheric pressure in the literature (reference 4). The measurements reported here were made primarily to check the behavior of dc glow discharges under the same conditions that the rf discharges were examined, i.e., with the same electrodes and cooling. The measured quantities are voltage and current densities.

(1) Voltage Measurements

The voltage was measured with a precision voltmeter, accuracy ± 3 volts. The voltage as a function of electrode distance is given in Figure A1 for two discharge currents. This measurement was made with plane parallel copper electrodes, which were water cooled. The voltage varies somewhat with time, the amount of variation being ± 3%.

The minimum voltage for very small electrode separations ($d \leq 0.025$mm) was found to be 275 V.

The voltages found for several different electrode materials were listed in section IV, d.

(2) Current Density Measurements

The current density J is defined as the quotient of current and the electrode area covered by the blue negative glow. The values found for J at different values of current are the following:

I = 100 millamps J = 8.0 amp/cm^2

I = 200 millamps J = 7.9 amp/cm^2

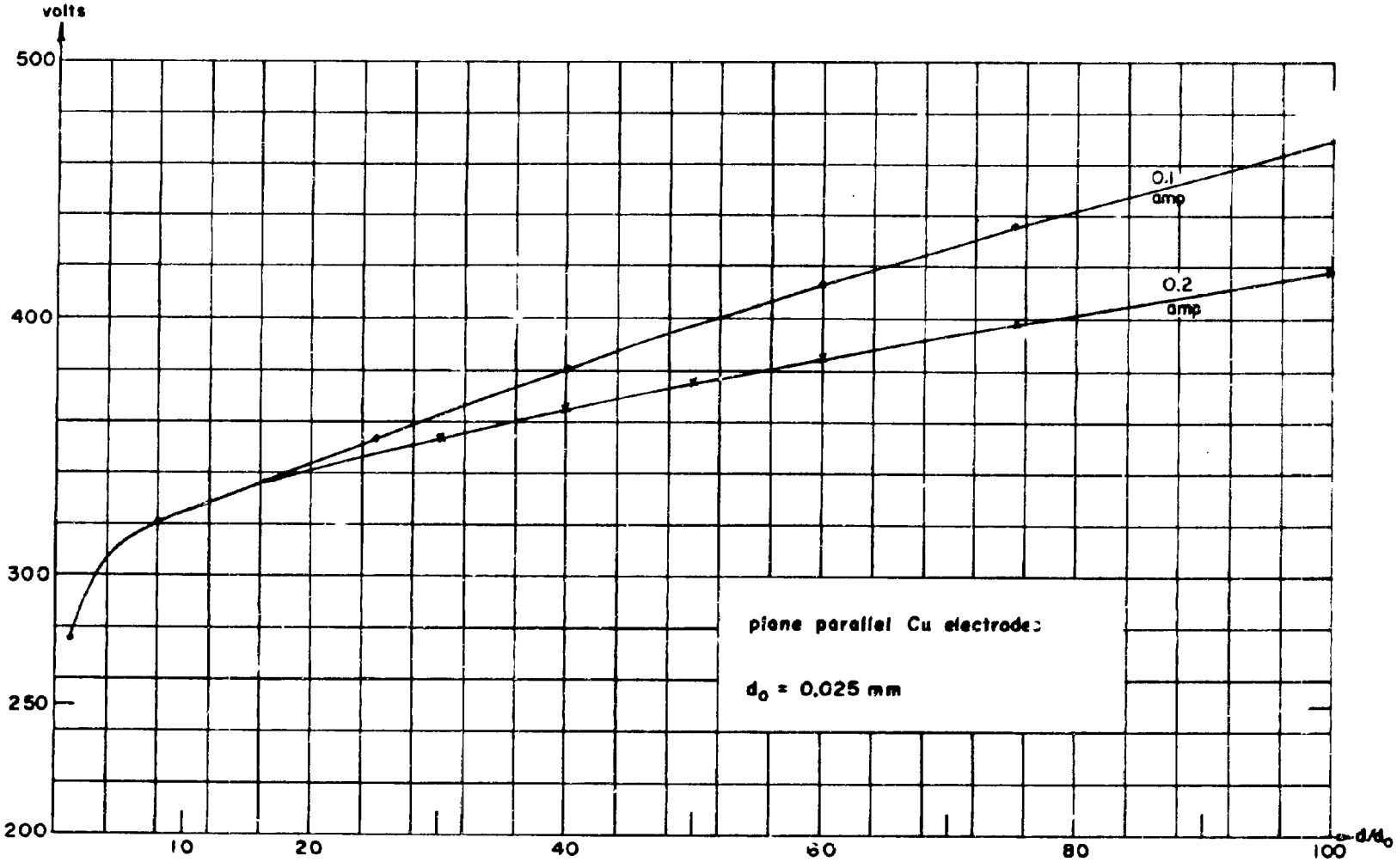

FIGURE A1 VOLTAGE NECESSARY TO MAINTAIN dc GLOW DISCHARGE

APPENDIX B

Distribution

HERO Dictribution List II
DDC (20)
NASA (5)

Local
W
T
WX
WD
WH
WHH
WHR
WHY
WHX (15)
WH-2
MAL (5)
WH-3

DOCUMENT CONTROL DATA - R & D

(Security classification of title, body of abstract and indexing annotation must be entered when the overall report is classified)

ORIGINATING ACTIVITY (Corporate author)	2a. REPORT SECURITY CLASSIFICATION
U. S. Naval Weapons Laboratory	UNCLASSIFIED
	2b. GROUP

3. REPORT TITLE

ELECTRICAL PROPERTIES OF RADIO FREQUENCY GLOW DISCHARGES IN AIR AT ATMOSPHERIC PRESSURE

4. DESCRIPTIVE NOTE (Type of report and inclusive dates)

5. AUTHOR(S) (First name, middle initial, last name)

H. A. Schwab

6. REPORT DATE	7a. TOTAL NO. OF PAGES	7b. NO. OF REFS
October 1967	59	

8a. CONTRACT OR GRANT NO.	9a. ORIGINATOR'S REPORT NUMBER(S)
b. PROJECT NO.	2124
c.	9b. OTHER REPORT NO(S) (Any other numbers that may be assigned this report)
d.	

10. DISTRIBUTION STATEMENT

Distribution of this document is unlimited.

11. SUPPLEMENTARY NOTES	12. SPONSORING MILITARY ACTIVITY

13. ABSTRACT

Gas discharges maintained by radio frequency power were examined in the frequency range 1-25 Mc/s. The discharges were maintained in air at atmospheric pressure between water cooled metal electrodes. The discharges were made symmetric by using two electrodes alike in shape and material.

Important discharge quantities such as the voltage necessary to maintain the discharge, current density, and dissipated power were measured. The minimum instantaneous value of voltage necessary to maintain a discharge was found to be 270 volts. The current density is largely independent of current and has a value of 30 amps/cm^2 (determined by using the peak discharge current). A minimum power of 4 watts is necessary to maintain a discharge.

The influence of current amplitude, frequency, electrode distance, and other parameters on discharge voltage and current density was examined. Both voltage and current density were found to be essentially independent of frequency in the frequency range considered.

Furthermore it was found that a number of properties of the type of discharge described in this report are analogous to the corresponding properties of dc glow discharges.

DD FORM 1 NOV 65 1473 (PAGE 1)

S/N 0101-807-6811

UNCLASSIFIED

Security Classification

A-31408